Earth-Science Reviews 107 (2011) 375–397

Contents lists available at ScienceDirect

Earth-Science Reviews

journal homepage: www.elsevier.com/locate/earscirev

Sveconorwegian massif-type anorthosites and related granitoids result from post-collisional melting of a continental arc root

J. Vander Auwera [a,*], O. Bolle [a], B. Bingen [b], J.-P. Liégeois [c], M. Bogaerts [a], J.C. Duchesne [a], B. De Waele [d], J. Longhi [e]

[a] UR Pétrologie, Géochimie endogènes et Pétrophysique (B20), Université de Liège, B-4000 Sart Tilman, Belgium
[b] Geological Survey of Norway, 7491 Trondheim, Norway
[c] Royal Museum of Central Africa, B-3080 Tervuren, Belgium
[d] SRK Consulting, 10 Richardson Street, West Perth, WA 6005, Western Australia
[e] Lamont-Doherty Earth Observatory, Palisades, NY, USA

ARTICLE INFO

Article history:
Received 3 November 2009
Received in revised form 28 October 2010
Accepted 15 April 2011
Available online 21 April 2011

Keywords:
Proterozoic massif-type anorthosites
Jotunites
Ferroan granites
Post-collisional magmatism
Sveconorwegian orogen
Lower continental crust

ABSTRACT

Two magmatic suites were emplaced during the post-collisional evolution of the Sveconorwegian orogeny: an Anorthosite–Mangerite–Charnockite suite (AMC suite), and an hornblende- and biotite-bearing granitoids suite (HBG suite). The AMC suite is exclusively located in the westernmost and warmest part of the orogen, in granulite facies gneisses, whereas the HBG suite intruded in the rest of the orogen, but not in the granulite domain. New U–Pb zircon geochronological data confirm previous age determinations: 970–932 Ma (HBG suite) and 933–916 Ma (AMC suite).

The mafic facies of the two post-collisional magmatic suites have similar geochemical compositions but the HBG differentiation trend displays higher CaO, Sr, U and Th as well as lower K_2O and FeO_t/MgO than the AMC differentiation trend. The HBG suite is hydrous and has a broadly higher fO_2 whereas the AMC suite is anhydrous.

The inferred parent magmas of both suites have overlapping initial Sr, Nd and Pb isotopic compositions. With increasing differentiation, the two trends point towards two different crustal contaminants. Together with the recent recognition of a major crustal shear zone located just east of the AMC suite, this difference suggests that the suites were emplaced in two different lithotectonic units.

Using published experimental constraints and geochemical modeling, we suggest that the mafic facies of both suites were produced by partial melting of lower crustal sources which were previously underplated, probably during the evolution of a long-lasting convergent margin. Later, these lower crustal sources were modified by the regional granulite facies metamorphism (1.035 to 0.97 Ga) prevailing in the westernmost part of the orogen, thus producing an anhydrous lower crustal source for the AMC suite.

Accordingly, we conclude that the Sveconorwegian massif-type anorthosites result from partial melting of the continental arc root. This process, if accepted for other AMCG (Anorthosite–Mangerite–Charnockite–Granite) complexes, was possible in the Proterozoic because of a sufficiently high temperature, but not in the Archean because in subduction zones the main transfer to the crust was then felsic (tonalites, granodiorites) and not basaltic. We thus further suggest that the onset of massif-type anorthosites at the beginning of the Proterozoic may mark the time when plate tectonics began to operate in a similar way as today.

Contents

* Corresponding author. Tel.: +32 4 3662253; fax: +32 4 3662029.
E-mail addresses: jvdauwera@ulg.ac.be (J. Vander Auwera), olivier.bolle@ulg.ac.be (O. Bolle), bernard.bingen@ngu.no (B. Bingen), jplieg@ulb.ac.be (J.-P. Liégeois), jc.duchesne@ulg.ac.be (J.C. Duchesne), longhi@ldeo.columbia.edu (J. Longhi).

0012-8252/$ – see front matter © 2011 Elsevier B.V. All rights reserved.
doi:10.1016/j.earscirev.2011.04.005

1. Introduction

Massif-type anorthosites have long been recognized as magmatic rocks typical of the Proterozoic (e.g. Ashwal, 1993; Vigneresse, 2005). U–Pb zircon and baddeleyite ages indicate that this magmatism was produced from 2.12 Ga (Arnanunat Plutonic Suite: Hamilton et al., 1998; Ryan et al., 1999) to 0.93 Ga (Rogaland Anorthositic Suite: Schärer et al., 1996). Anorthosites are most frequently associated with a series of rocks, many of which are orthopyroxene (opx)-bearing: mangerites (opx-bearing monzonites), charnockites (opx-bearing granites), granites and also jotunites (opx-bearing monzodiorites), ferrodiorites, gabbros and troctolites (e.g. Wiebe, 1992). The association prompted Emslie (1985) and Emslie et al. (1994) to group these rocks into an AMCG (Anorthosite–Mangerite–Charnockite–Granite) suite. The origin of these anorthositic plutons, where plagioclase is the dominant phase (75% to 95%), has been the subject of lasting petrological debates. Their restricted time occurrence has long suggested that anorthosites can provide important clues on the global evolution of the Earth through time. The composition of the parent magmas of AMCG suites has also been discussed extensively and several magma types have been considered: high-Al gabbros (Emslie, 1978; Duchesne et al., 1985a; Fram and Longhi, 1992; Charlier et al., 2010), jotunites (Duchesne et al., 1974; Demaiffe et al., 1986; Duchesne, 1990; Vander Auwera et al., 1998; Longhi et al., 1999), and troctolitic basalts (Nolan and Morse, 1986). Until recently, most authors favored a mantle origin (e.g. Morse, 1982; Olsen and Morse, 1990; Ashwal, 1993; Emslie et al., 1994; Frost and Frost, 1997; Markl and Hohndorf, 2003) but emerging geochemical (Duchesne et al., 1985b; Duchesne, 1990; Bédard, 2001; Corfu, 2004; Bédard, 2010), isotopic (Stein et al., 1998; Schiellerup et al., 2000; Wiszniewska et al., 2002; Duchesne et al., 2007) and phase equilibria considerations (Longhi et al., 1999; Longhi, 2005) are now supporting a lower crustal source in agreement with earlier work (Simmons and Hanson, 1978; Taylor et al., 1984). In the Sveconorwegian orogen of Fennoscandia, U–Pb zircon and Re–Os molybdenite ages on magmatic and metamorphic rocks (Bingen and van Breemen, 1998a, 1998b; Möller et al., 2002; Bingen and Stein, 2003; Tomkins et al., 2005; Bingen et al., 2006; Andersen et al., 2007a) have provided precise constraints on the evolution of this orogen, confirming that massif-type anorthosites were emplaced during its post-collisional period (Bingen et al., 2008), just after a series of abundant granitoids. Here, we present arguments based on detailed petrological and geochemical studies to support the hypothesis that their parent magmas were produced by partial melting of lower crustal sources that were previously underplated probably during the evolution of a long-lasting convergent margin.

2. Geological outline of Southwest Scandinavia

The Sveconorwegian orogen is located along the western margin of Fennoscandia, and is currently interpreted as an eastward extension of the Grenville orogen of Laurentia. It possibly resulted from the collision between Fennoscandia and a large unknown craton, maybe Amazonia, at the end of the Mesoproterozoic, contributing to the assembly of Rodinia (recent reviews in Bingen et al., 2008; Bogdanova et al., 2008). It is made up of one parautochthonous segment, the Eastern Segment, and two main allochthonous terranes, the Idefjorden and Telemarkia terranes (Fig. 1). The Eastern Segment mainly consists of reworked granitoids of the 1.85–1.65 Ga Transscandinavian Igneous Belt, while the Idefjorden and Telemarkia terranes are mainly made up of Mesoproterozoic metasedimentary, metavolcanic and metaplutonic rocks. Several sectors have been recognized in the Telemarkia terrane: Rogaland–Vest Agder, Suldal, Hardangervidda and Telemark. The Bamble–Kongsberg terrane is interpreted by Bingen et al. (2005) and Bingen et al. (2008) as a minor collision zone between the Idefjorden and Telemarkia terranes.

Based on available geochronology and metamorphic petrology, Bingen et al. (2008) subdivided the history of the Sveconorwegian orogeny into four phases. The *Arendal phase* (1.14–1.08 Ga) corresponds to the collision between the Telemarkia and Idefjorden terranes, producing the Bamble–Kongsberg tectonic wedge. After a period of quiescence (1.08–1.05 Ga), the *Agder phase* (1.05–0.98 Ga) records the collision between Fennoscandia and Amazonia (?) resulting in tectonic imbrication and major crustal thickening. In Telemarkia, metamorphism related to this phase took place between 1.035 and 0.97 Ga (M1 phase in Rogaland–Vest Agder; see below) and increased in intensity southwestwards from amphibolite-facies to granulite-facies (Fig. 1B). The *Falkenberg phase* (0.98–0.97 Ga) bears evidence of crustal thickening and final convergence in the Eastern Segment, in the form of high-grade metamorphism and the presence of 972 ± 14 Ma (retro)eclogites (Johansson et al., 2001) combined with initiation of regional decompression in Rogaland–Vest Agder. During the *Dalane phase* (0.97–0.90 Ga), gravitational collapse of the orogen occurred together with emplacement of the postcollisional magmatism.

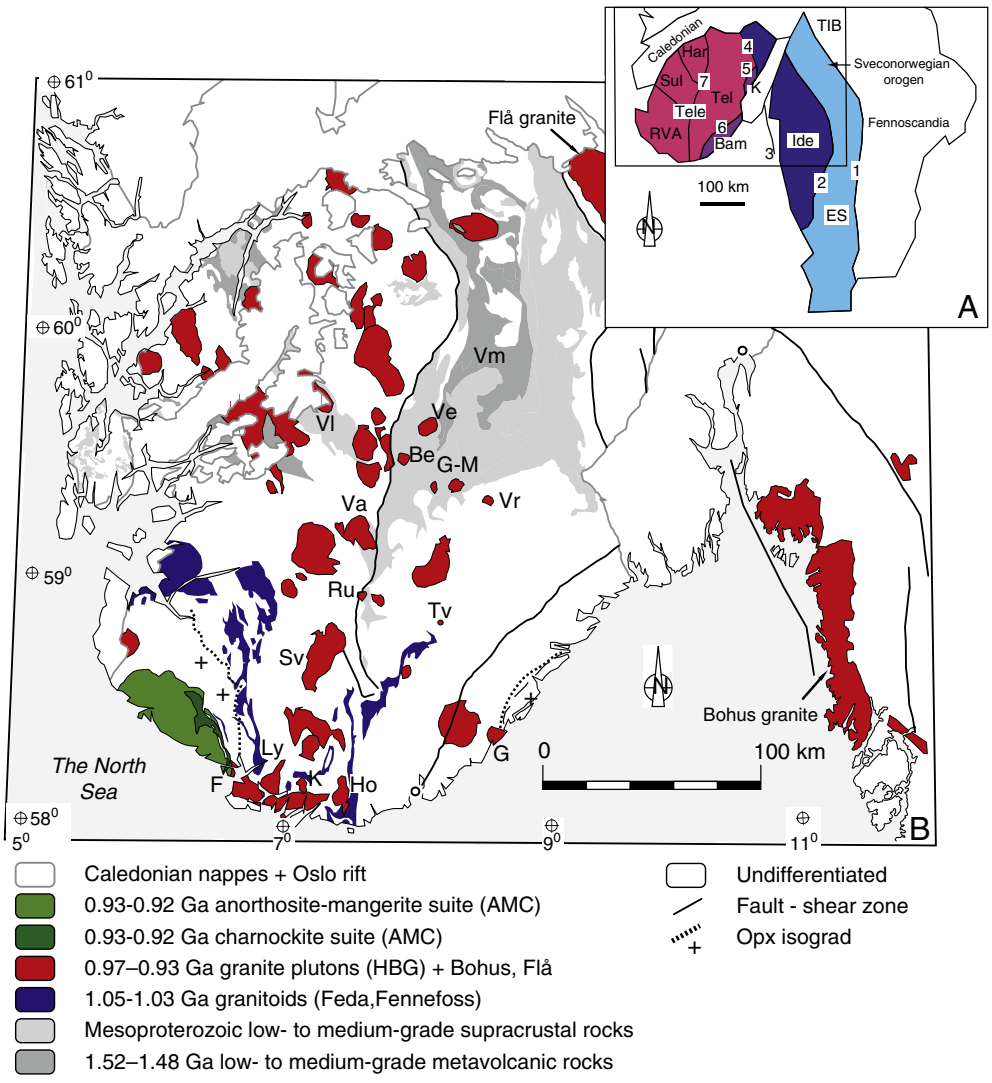

Fig. 1. (A) Situation map of SW Scandinavia and lithotectonic domains as defined by Bingen et al. (2005) and Bingen et al. (2008). Tele: Telemarkia terrane (RVA: Rogaland–Vest Agder; Sul: Suldal; Har: Hardangervidda; Tel: Telemark), Ide: Idefjorden terrane, ES: Eastern Segment. Bam: Bamble, K: Kongsberg. 1. Sveconorwegian frontal deformation zone; 2: Mylonite zone; 3: Östfold–Marstrand boundary zone; 4: Åmot–Vardefjell shear zone; 5: Saggrenda–Sokna shear zone; 6: Kristiansand–Porsgrunn shear zone; 7: Mandal–Ustaoset fault and shear zone (after Bingen et al., 2005). (B) Geological sketch map of SW Scandinavia showing the Sveconorwegian post-collisional magmatic suites as well as the orogenic granitoids. F: Farsund, G: Grimstad, Ly: Lyngdal, K: Kleivan, Ho: Holum, Sv: Svöfjell, Ru: Rustfjellet, Tv: Tovdal, Va: Valle, Be: Bessefjellet, Ve: Verhuskjerringi, Vr: Vrådal. The position of the main Mesoproterozoic mafic magmatism (Vl: Valldal (1.26 Ga), G–M: Gjuve–Morgedal (1.16 Ga), Vm: Vemork (1.5 Ga)) and of the Opx-in isograd related to the Sveconorwegian regional metamorphism are also shown (after Bingen et al., 2008).

In Rogaland–Vest Agder, petrological and geochronological data (Maijer, 1987; Bingen and van Breemen, 1998b; Möller et al., 2002; Tomkins et al., 2005) indicate a sequence of three metamorphic phases. The M1 phase corresponds to the Sveconorwegian regional metamorphism dated at 1.035 to 0.97 Ga (Bingen and van Breemen, 1998b). The M2 phase is a high- to ultra high-T thermal event associated with intrusion of the AMC suite of Rogaland (Fig. 1) at 0.93 Ga (Schärer et al., 1996). Finally, M3 is post-M2 cooling that led to progressive reequilibration of parageneses (Rietmeijer, 1984; Maijer, 1987). Thus, high grade conditions persisted for more than 100 Ma (1.035–0.90 Ga) in Rogaland–Vest Agder through two successive granulite-facies events (M1 at 1.035–0.97 Ga and M2 at 0.93–0.92 Ga) (see Bingen et al., 2008). Four main isograds have been recognized. With increasing grade of metamorphism from NE to SW, these isograds are: cpx-in among granodioritic gneisses, opx-in in granitic gneisses, osumilite-in in paragneisses and pigeonite in granitic gneisses (Fig. 2A). These isograds are not coeval: the cpx-in isograd is related to the 0.93 Ga thermal event (Bingen and van Breemen, 1998a; Bingen and Stein, 2003), opx-bearing assemblages have been recognized in both M1 and M2 phases, and available geochronological data suggest that the osumilite-in and pigeonite-in isograds are linked to the 0.93 Ga metamorphic phase (Möller et al., 2002). However, Bingen and Stein (2003) pointed out that the pressure–temperature conditions necessary for osumilite crystallization are similar to those of the molybdenite + orthopyroxene + garnet assemblage which they dated at 0.97 Ga. This observation gives strong support to the hypothesis that osumilite may have been formed during the regional metamorphism at 0.97 Ga. Moreover, the 973 ± 4 Ma age obtained for the molybdenite + orthopyroxene + garnet assemblage in the Ørsdalen district (located on the opx-in isograd, about 15 km north-east of the AMC suite) unambiguously proves the existence of a granulite-facies basement in Rogaland before the emplacement of the post-collisional magmatism. Additionally, these authors noted that monazite from granulite samples collected west of the osumilite and pigeonite isograds gives ages between 1018 ± 2 and 972 ± 2 Ma indicating that the main granulite-facies in Rogaland took place between 1.03 and 0.97 Ga during regional metamorphism. It is also possible that the M2 phase was not a simple contact

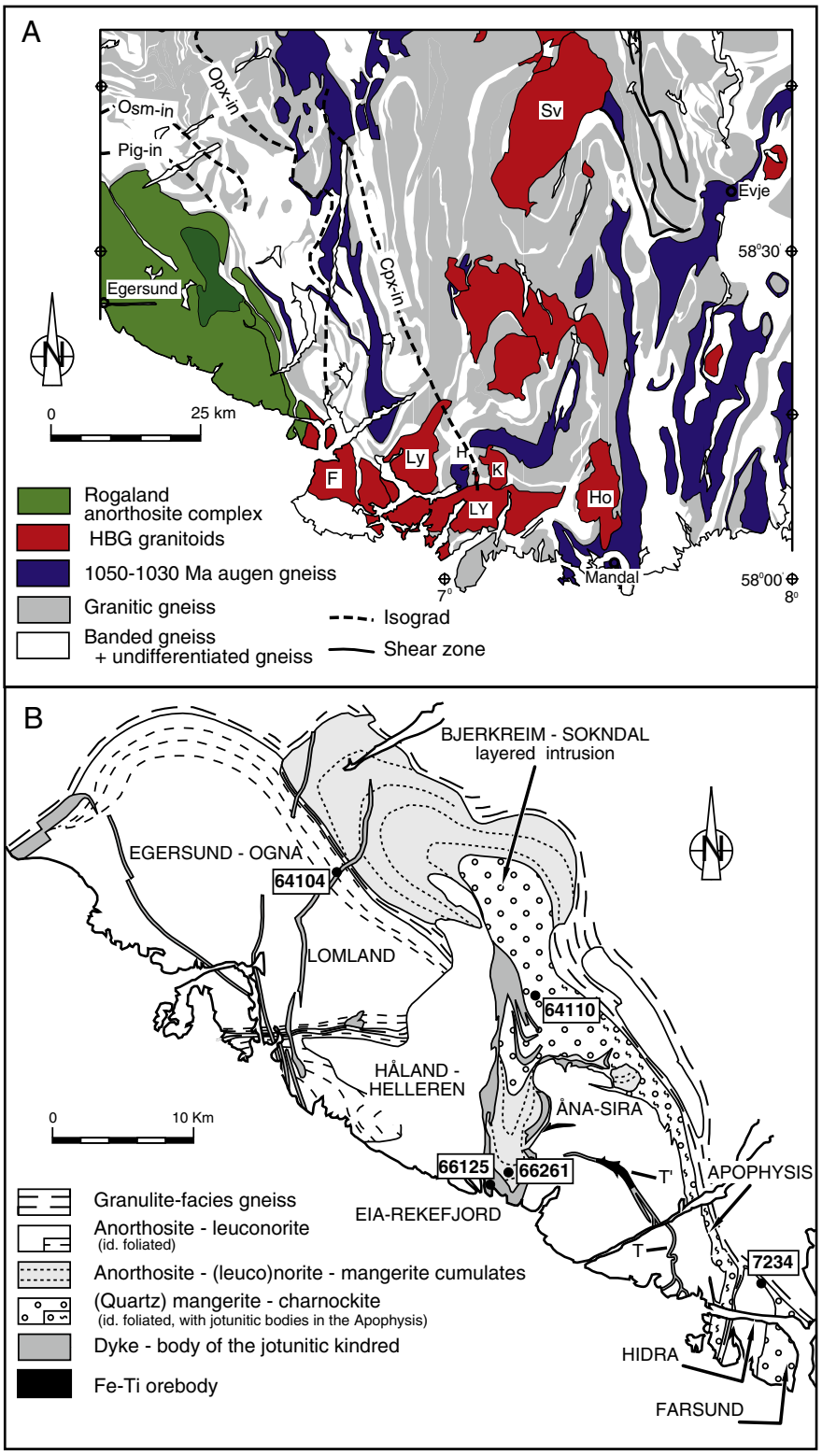

Fig. 2. (A) Geological sketch map of southwest Rogaland showing the Rogaland Anorthosite Complex and the location of the Lyngdal and Skoland gabbronorites (H) (F: Farsund, Ly: Lyngdal, Ho: Holum, K: Kleivan, Sv: Svöfjell) (after Falkum, 1982 and Bingen et al., 2006). (B) Geological map of the Rogaland anorthositic province. T = Tellnes dyke, T′ = Tellnes ore body (after Michot and Michot, 1969; Falkum, 1982; Bolle et al., 2003a). The position of the new geochronological samples is also shown.

metamorphism. Indeed, titanite ages from Rogaland–Vest Agder and Telemark are tightly grouped at 918 ± 2 Ma and 913–901 Ma suggesting that a homogeneous regional cooling took place after the M2 metamorphic phase associated with the intrusion of the Rogaland intrusive complex at 0.93 Ga (Bingen and van Breemen, 1998b).

Voluminous magmatism took place before and during the Sveconorwegian orogeny. In the Telemarkia terrane, the first recorded magmatic event took place at around 1.5 Ga forming abundant granitoids, and felsic and mafic volcanic rocks (Bingen et al., 2005). It includes the bimodal Rjukan Group in Telemark (Vemork — Vm — mafic volcanics in

Fig. 1B) (Brewer and Menuge, 1998). The lack of older exposed magmatic rocks in the Telemarkia terrane does not exclude the presence of older crustal components (in metasediments) and/or of a concealed older lower crust (Andersen et al., 2001). Subsequent events of magmatism occurred at 1.28–1.26 Ga (Valldal —Vl — mafic volcanics in Fig. 1B) (Bingen et al., 2002; Brewer et al., 2004), at 1.21–1.20 Ga (granite plutonism: Heaman and Smalley, 1994; Andersen et al., 2007b), and between 1.17 and 1.14 Ga (Gjuve and Morgedal — G–M — mafic volcanics in Fig. 1B) (Zhou et al., 1995; Brewer et al., 2002; Laajoki et al., 2002). Abundant "orogenic" phenocryst-bearing granodiorites of the Feda and Fennefoss suites, discussed below, were intruded at 1.05–1.03 Ga (Bingen and van Breemen, 1998a) and are now deformed to augen gneiss (Fig. 2B). They possibly reflect a final subduction episode. Syn-collisional magmatism in the 1.03–0.97 Ga interval is apparently lacking in the Telemarkia terrane, but abundant post-collisional magmatism occurred mainly between 0.97 and 0.92 Ga. It includes the two magmatic suites which are the focus of this publication: the hornblende–biotite granitoids (HBG) suite, mainly occurring as a plutonic belt in the central part of the Telemarkia terrane east of the Opx-in isograd (0.97–0.93 Ga) (Andersson et al., 1996; Andersen et al., 2001; Bogaerts et al., 2003a; Vander Auwera et al., 2003), and the Rogaland Anorthosite–Mangerite–Charnockite suite, here referred to as an AMC suite as true granites are lacking, located in the granulitic gneisses west of the Opx-in isograd (e.g. Michot and Michot, 1969; Duchesne et al., 1985a) (0.93–0.92 Ga; Figs. 1B and 2B).

3. Analytical methods

To complement available database (see Section 4.3), additional analyses have been carried out. Firstly, trace elements (Table 1) and Sr, Nd, Pb isotopic data (Tables 2 and 3) were acquired on three fine-grained amphibolitic enclaves of the Feda augen gneiss: samples BB17a, BB120b and BB82b. These samples were crushed on a steel anvil and then ground into powders using planetary agate ball mills. Secondly, U–Pb geochronological data were acquired on zircon from 6 samples of the AMC and HBG suites to better constrain the timespan of these two postcollisional suites.

3.1. Trace element analyses

Rb and Sr have been measured with an ARL 9400 XP X-ray fluorescence (University of Liège) on pressed powder pellets with a precision better than 5% (Bologne and Duchesne, 1991). Other trace element concentrations were measured by ICPMS at MRAC (Tervuren, Belgium). 0.3 g of sample mixed with 0.9 g of lithium tetraborate were fused at 1000 °C for 1 h. The glass was then dissolved in 5% HNO3. The calibrations were performed using both synthetic solutions (mixtures of one given set of elements at 2, 5, 10 ppb) and international rock standards (BHVO-1, W1, GA, ACE). For these elements, the precision ranges from 5 to 10% (see Navez, 1995).

3.2. Sr and Nd isotopes

After acid dissolution of the sample, and Sr and/or Nd separation on ion-exchange resin, Sr isotopic compositions were measured on Ta single filaments and Nd isotopic compositions on triple Ta–Re–Ta filaments in a thermal ionization mass spectrometer (VG Sector 54) from the Isotope Geology division at MRAC, Tervuren. Repeated measurements of Sr and Nd standards have shown that the between-run error is better than 0.000015 (2σ). During the course of this study, the NBS987 standard yielded a value for $^{87}Sr/^{86}Sr = 0.710281 \pm 0.000007$ (2σ on the mean of the 4 standards measured for each set of 16 samples, normalized to $^{86}Sr/^{88}Sr = 0.1194$) and the Rennes Nd standard, a value of $^{143}Nd/^{144}Nd = 0.511961 \pm 0.000006$ (2σ on the mean of the 4 standards measured for each set of 16 samples, normalized to $^{146}Nd/^{144}Nd = 0.7219$). All the ratios of the unknown have been normalized to the recommended values of 0.710250 for NBS987 and 0.511963 for Nd Rennes standard (corresponding to a La Jolla value of 0.511866). The decay constant for ^{87}Rb (1.42×10^{-11} y^{-1}) was taken from Steiger and Jäger (1977) and for ^{147}Sm (6.54×10^{-12} y^{-1}) from Lugmair and Marti (1978). Nd T_{DM} model ages have been calculated following Vervoort et al. (2000).

3.3. Pb isotopes

The samples were dried at 40 °C and crushed in an agate mortar. About ~50 mg of powder were dissolved either in closed Teflon vessel enclosed in steel jackets using $HF + HNO_3$ at 180 °C, or in Savillex® beakers using concentrated $HF + HNO_3$ at 130 °C for 48 h, followed by evaporation, addition of 6 M HCl, second evaporation and final dissolution in HBr 0.5 N. Lead separation was performed using successive acid elutions on anionic resin (AG1-X8) (for further details see Weis et al., 2006). The entire chemical purification was carried out in a class 100 laminar air flow cabinet. Collected lead samples were then evaporated and dried residues were dissolved in 100 µl of concentrated HNO_3, evaporated and finally dissolved in 1.5 ml of 0.05 M HNO_3. Tl was added to each sample and standard, to control the instrumental mass fractionation. Solutions were prepared so as to obtain a Pb/Tl ratio of 4 or 5, a signal of 100 mV in the axial collector (^{204}Pb) and to match the Pb and Tl concentrations of the standard (200 ppb Pb and 50 ppb Tl). Lead isotopes were measured at Université Libre de Bruxelles (Belgium) using a Nu Plasma Multi-Collector Inductively Coupled Plasma Mass Spectrometer (MC-ICP-MS) upgraded with an Edwards E2M80 high performance interface pump. The instrument was operated under wet plasma conditions with a Glass Expansion MicroMist nebulizer at a

Table 1
Major (wt.%) and trace element (ppm) analyses of amphibole-rich enclaves of the Feda suite.

	BB 17a	BB 82b	BB 120b
SiO_2	58.81	48.35	52.07
TiO_2	1.96	1.24	0.92
Al_2O_3	14.07	15.93	15.92
Fe_2O_3	5.50	4.12	6.23
FeO	3.98	8.25	5.42
FeO_t	8.93	11.96	11.03
MnO	0.09	0.14	0.16
MgO	2.67	8.83	5.88
CaO	5.23	9.71	7.88
Na_2O	3.27	2.43	3.35
K_2O	2.51	1.26	1.82
P_2O_5	0.59	0.23	0.33
Ni	14	117	37
V	149	211	195
Rb	66	77	30
Sr	470	222	787
Y	38	20	42
Zr	393	88	159
Nb	16	1	5
Ba	1051	103	753
La	91	7	35
Ce	192	18	88
Pr	24	2.1	10
Nd	85	9.2	38
Sm	14	2.2	7.2
Eu	2.9	1.0	2.1
Gd	12	2.9	7.0
Dy	6.7	3.2	6.4
Ho	1.2	0.63	1.3
Er	3.2	1.9	3.8
Yb	2.4	1.8	4.1
Lu	0.37	0.25	0.63
Hf	11	1.7	2.7
Ta	0.87	0.00	0.11
Pb	17	7.6	16
Th	12	1.1	1.1
U	0.75	0.66	0.35

Major elements and Ni, Rb, Sr, Zr (XRF data) are from Bingen (1988).
Other trace elements by ICP-MS (this work).

Table 2
Rb/Sr and Sm/Nd isotopic data of the Feda mafic facies.

Sample	Description	Rb	Sr	$^{87}Rb/^{86}Sr$	$^{87}Sr/^{86}Sr$	2σ	$(^{87}Sr/^{86}Sr)$ 0.93 Ga	$(^{87}Sr/^{86}Sr)$ 1.05 Ga	Sm	Nd	$^{147}Sm/^{144}Nd$	$^{143}Nd/^{144}Nd$	2σ	$(^{143}Nd/^{144}Nd)$ 0.93 Ga	εNd 0.93 Ga	$(^{143}Nd/^{144}Nd)$ 1.05 Ga	εNd 1.05 Ga	TDM (Ma)
BB117b	K enclave Feda	240	2374	0.2925	0.70753	2	0.70364	0.70314	31.3	220	0.0860	0.51195	4	0.51143	−0.3	0.51136	1.46	1432
BB81a	K enclave Feda	264	1713	0.4460	0.70959	3	0.70366	0.70289	31.2	221	0.0854	0.51194	2	0.51142	−0.4	0.51135	1.35	1436
BB157	K enclave Feda	109	3735	0.0844	0.70495	3	0.70383	0.70368	42.1	302	0.0825	0.51190	1	0.51140	–0.8	0.51133	0.71	1451
BB82b	Amphibole-rich enclave Feda	77	222	1.0044	0.716447	8	0.703095	0.701359	2.2	9.2	0.1446	0.512472	8	0.511590	3.0	0.511476	3.76	1495
BB120b	Amphibole-rich enclave Feda	30	787	0.1103	0.705469	8	0.704003	0.703813	7.2	38	0.1146	0.512104	7	0.511405	−0.6	0.511315	0.66	1607
BB17	Amphibole-rich enclave Feda	66	470	0.4064	0.710212	7	0.704810	0.704107	14	85	0.0996	0.511958	8	0.511350	−1.7	0.511272	−0.21	1590

Isotopic and geochemical data for samples BB117b, BB81a, BB157 are from Bingen et al. (1993) and Bingen (1989). Parameters used in the calculations of initial ratios: $^{187}Rb = 1.42 \times 10^{-11}$ per year, $^{147}Sm = 6.54 \times 10^{-12}$ per year and CHUR present ratios are $^{143}Nd/^{144}Nd = 0.512638$ and $^{147}Sm/^{144}Nd = 0.1967$. Model ages are calculated according to Vervoort et al. (2000) (present day depleted mantle values: $^{143}Nd/^{144}Nd = 0.513151$ and $^{147}Sm/^{144}Nd = 0.2137$).

Table 3
Pb isotopic composition of the Feda mafic facies.

Sample	Description	$^{206}Pb/^{204}Pb$	$^{207}Pb/^{204}Pb$	$^{208}Pb/^{204}Pb$	Pb (ppm)	U (ppm)	Th (ppm)	$(^{206}Pb/^{204}Pb)_{1.05\ Ga}$	$(^{207}Pb/^{204}Pb)_{1.05\ Ga}$	$(^{208}Pb/^{204}Pb)_{1.05\ Ga}$	$(^{206}Pb/^{204}Pb)_{0.93\ Ga}$	$(^{207}Pb/^{204}Pb)_{0.93\ Ga}$	$(^{208}Pb/^{204}Pb)_{0.93\ Ga}$
BB117b	K enclave Feda	19.502	15.660	38.524	33	6.3	16.9	17.32	15.50	36.70	17.59	15.53	36.70
BB82b	Amphibole-rich enclave Feda	17.921	15.521	37.003	8	0.66	1.1	16.97	15.45	36.50	17.09	15.46	36.56
BB120b	Amphibole-rich enclave Feda	17.151	15.460	36.586	16	0.35	1.1	16.92	15.44	36.36	16.94	15.45	36.39
BB17	Amphibole-rich enclave Feda	17.556	15.507	37.363	17	0.75	12.1	17.06	15.47	34.87	17.12	15.48	35.16
BB17 (duplicate)	Amphibole-rich enclave Feda	17.556	15.508	37.362	17	0.75	12.1	17.06	15.47	34.87	17.12	15.48	35.16

Isotopic and geochemical data for sample BB117b are from Bingen et al. (1993) and Bingen (1989). Parameters used in the calculations of initial ratios: $^{238}U = 1.55125 \times 10^{-10}$ per year, $^{235}U = 9.8485 \times 10^{-10}$ per year and $^{232}Th = 4.9475 \times 10^{-11}$ per year.

sample uptake of 100 μl/min, fitted into a Peltier cooled (5 °C) Glass Expansion Cinnabar cyclonic spray chamber. Standard narrow-angle nickel cones were used. The certified reference material NBS981 (NIST) was repeatedly measured (n = 9) during the analytical session. Lead isotope ratios were obtained after mass bias correction using the exponential law and application of the standard bracketing method with the recommended values of Galer (1999). The NBS981 isotopic ratios were reproducible with mean values of 36.7162 ± 0.0040 (2σ) for the $^{208}Pb/^{204}Pb$ ratio, 15.4972 ± 0.0014 for the $^{207}Pb/^{204}Pb$ ratio, 16.9415 ± 0.0015 for $^{206}Pb/^{204}Pb$ ratio. These values are in good agreement with the long term mean internal laboratory measurements (n ≈ 750), which are 36.7147 ± 0.0063 (2σ), 15.4968 ± 0.0022, 16.9402 ± 0.0024.

3.4. U–Pb zircon geochronology

U–Pb geochronological data were collected by ion microprobe (Secondary Ion Mass Spectrometry, SIMS). Zircon grains were hand selected and mounted in epoxy resin, together with reference zircon chips. The grains were polished approximately to half thickness. Cathodoluminescence images (CL) were collected in a scanning electron

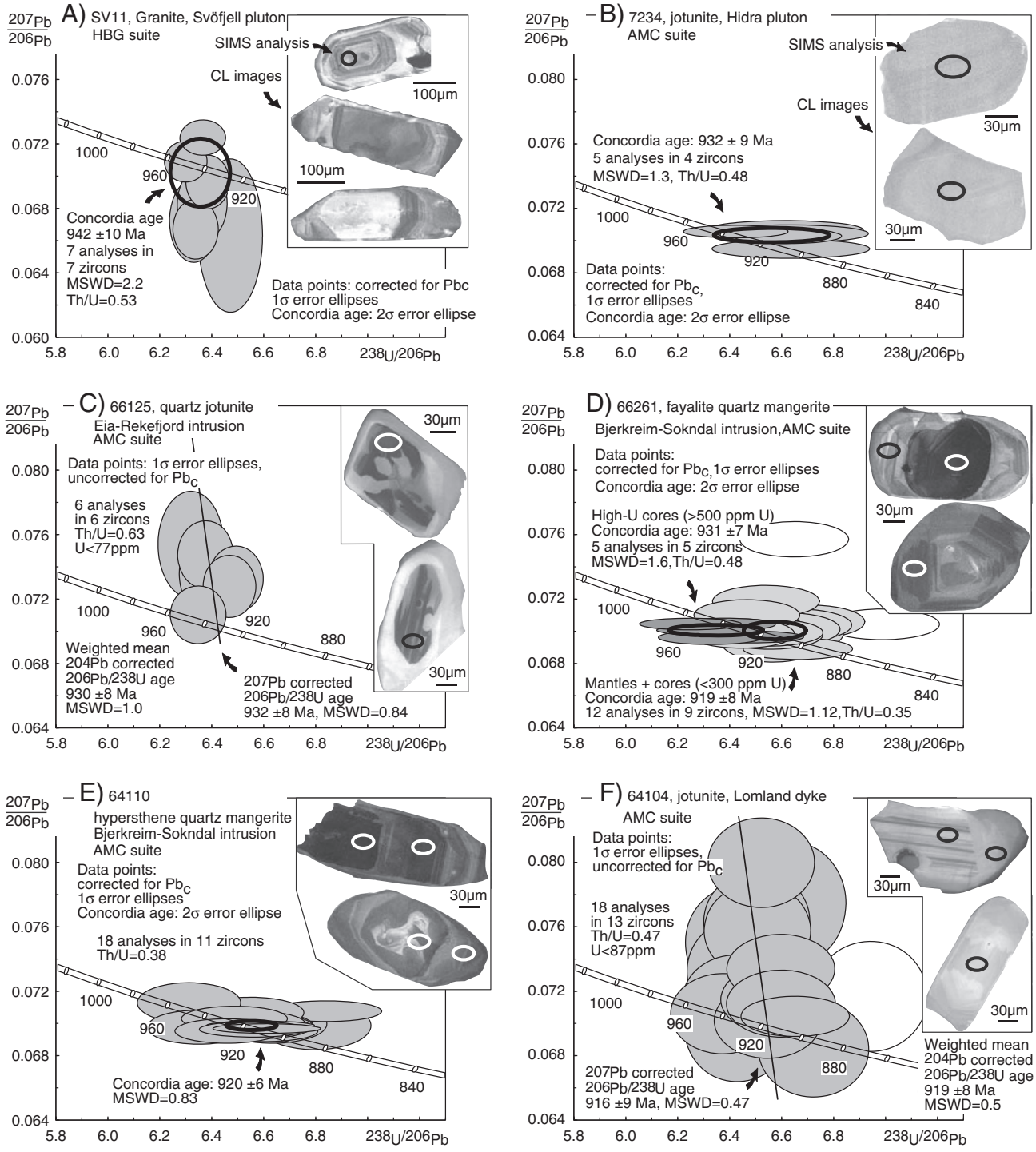

Fig. 3. U–Pb data on zircon from several intermediate and felsic rocks of the HBG and AMC suites. Cathodoluminescence (CL) images of selected zircon grains with locations of SIMS analyses are shown for each sample.

Table 4
SIMS U–Pb geochronological data on zircon.

Id	Z	U	Th	206Pb	f	238U	±	207Pb	±	238U	±	207Pb	±	207Pb	±	206Pb	±	Co	206Pb	±	207Pb	±
				204Pb		206Pb	1σ	206Pb	1σ	206Pb	1σ	206Pb	1σ	235U	1σ	238U	1σ		238U	1σ	206Pb	1σ
					%		%		%		%		%		%		%		Ma		Ma	
1	2	ppm	ppm		3	4		4		5		5		5		5		6	5		5	
SV11, granite, Svöfjell pluton, HBG suite, S Ljosland, E: 406969, y: 6510493 (7, 8)																						
11-1		165	135	4113	0.4	6.307	0.9	.07012	1.0	6.334	0.9	.06663	1.9	1.45	2.1	.1579	0.9	.44	945	8	826	39
11-2		150	77	>1e6	0.0	6.362	0.9	.07236	1.0	6.362	0.9	.07236	1.0	1.58	1.4	.1573	0.9	.65	942	8	1010	22
11-3		188	75	8635	0.2	6.369	0.9	.07124	0.9	6.381	0.9	.06958	1.6	1.50	1.8	.1567	0.9	.48	938	8	916	33
11-4		112	63	4942	0.3	6.338	1.0	.07112	1.2	6.360	1.0	.06821	2.2	1.48	2.4	.1572	1.0	.41	941	9	875	46
11-5		133	54	3369	0.5	6.294	1.0	.07143	1.1	6.326	1.0	.06716	2.6	1.46	2.7	.1581	1.0	.36	946	9	843	53
11-6		189	87	29364	0.1	6.293	0.9	.07134	0.9	6.296	0.9	.07086	1.2	1.55	1.5	.1588	0.9	.59	950	8	953	24
11-7		62	42	2290	0.8	6.420	1.2	.07251	1.5	6.470	1.3	.06623	4.8	1.41	4.9	.1546	1.3	.26	927	11	814	100
7234, jotunite, Hidra pluton, Itland, E: 359100, y: 6460300, (7, 9)																						
1239-01a	c	657	325	517325	0.0	6.421	2.1	.07049	0.4	6.421	2.1	.07049	0.4	0.514	2.1	.1557	2.1	.98	933	18	943	8
1239-02a	c	481	194	72624	0.0	6.621	2.1	.07021	0.4	6.621	2.1	.07021	0.4	1.462	2.1	.1510	2.1	.98	907	18	934	9
1167-02a	c	801	411	64886	0.0	6.611	3.0	.07058	0.5	6.611	3.0	.07058	0.5	1.472	3.1	.1513	3.0	.98	908	26	945	11
1167-05a	c	623	309	37123	0.1	6.632	3.0	.06980	0.5	6.635	3.0	.06941	0.6	1.442	3.1	.1507	3.0	.98	905	26	911	12
1167-06a	c	672	332	109250	0.0	6.629	3.0	.07034	0.5	6.629	3.0	.07034	0.5	1.463	3.1	.1508	3.0	.99	906	26	938	11
66125, quartz jotunite, Eia-Rekefjord intrusion, Rekefjord, E: 339660, y: 6469000, (7, 9)																						
1168-05a	c	65	44	1721	1.1	6.373	1.1	.07469	1.9	6.443	1.1	.06634	3.6	1.420	3.7	.1552	1.1	.30	930	10	817	73
1168-06c	c	73	53	3252	0.6	6.345	1.1	.07095	1.7	6.381	1.1	.06652	2.7	1.437	2.9	.1567	1.1	.39	938	10	823	55
1168-18ax	c	9	5	443	4.2	5.967	1.2	.09225	5.0	6.230	1.4	.05944	16.2	1.316	16.3	.1605	1.4	.08	960	12	583	318
1168-19a	c	77	60	1957	1.0	6.466	1.0	.07272	1.8	6.528	1.0	.06536	3.1	1.380	3.2	.1532	1.0	.32	919	9	786	63
1168-21a	c	37	20	1378	1.4	6.380	1.1	.07349	2.4	6.468	1.2	.06301	5.5	1.343	5.6	.1546	1.2	.20	927	10	709	113
1168-22a	c	72	39	5061	0.4	6.491	1.1	.07319	1.9	6.491	1.1	.07319	1.9	1.555	2.2	.1541	1.1	.50	924	9	1019	37
1168-23a	c	54	34	4579	0.4	6.317	1.3	.07533	2.9	6.317	1.3	.07533	2.9	1.644	3.2	.1583	1.3	.41	947	12	1077	58
66261, fayalite quartz mangerite, Bjerkreim-Sokndal intrusion, Kvitefjell, E: 331900, y: 6475300 (7, 9)																						
1235-01a	c	1141	438	225677	0.0	6.314	2.1	.06999	0.3	6.314	2.1	.06999	0.3	1.528	2.1	.1584	2.1	.99	948	18	928	6
1235-01b	m	131	37	21051	0.1	6.566	2.1	.06943	1.4	6.566	2.1	.06943	1.4	1.458	2.5	.1523	2.1	.84	914	18	912	28
1235-02a	c	1014	435	25132	0.1	6.244	2.1	.07038	0.3	6.244	2.1	.07038	0.3	1.554	2.1	.1601	2.1	.99	958	19	939	7
1235-02b	m	157	51	10535	0.2	6.551	2.1	.06969	0.9	6.551	2.1	.06969	0.9	1.467	2.3	.1526	2.1	.93	916	18	919	18
1235-03a	c	153	77	51853	0.0	6.444	2.1	.06977	0.9	6.444	2.1	.06977	0.9	1.493	2.3	.1552	2.1	.92	930	18	922	18
1235-03b	m	128	37	19406	0.1	6.659	2.1	.07031	0.9	6.659	2.1	.07031	0.9	1.456	2.3	.1502	2.1	.91	902	18	937	19
1235-04a	c	131	61	17955	0.1	6.708	2.1	.07051	1.0	6.708	2.1	.07051	1.0	1.449	2.3	.1491	2.1	.91	896	18	943	20
1235-04b	m	158	37	100768	0.0	6.503	2.1	.06993	0.9	6.503	2.1	.06993	0.9	1.483	2.3	.1538	2.1	.91	922	18	926	19
1235-05a	m	276	87	34869	0.1	6.662	2.1	.06883	0.6	6.662	2.1	.06883	0.6	1.425	2.2	.1501	2.1	.96	902	18	894	13
1235-06a	c	1484	606	128895	0.0	6.372	2.1	.07034	0.4	6.372	2.1	.07034	0.4	1.522	2.1	.1569	2.1	.99	940	18	938	7
1235-06b	m	123	35	>1e6	0.0	6.616	2.1	.07004	1.0	6.616	2.1	.07004	1.0	1.460	2.3	.1511	2.1	.91	907	18	930	20
1235-07a	c	136	60	46647	0.0	6.628	2.1	.06978	1.1	6.628	2.1	.06978	1.1	1.452	2.4	.1509	2.1	.89	906	18	922	22
1235-07bx	m	145	45	31437	0.1	6.989	2.1	.07035	0.9	6.989	2.1	.07035	0.9	1.388	2.3	.1431	2.1	.92	862	17	939	18
1235-08a	c	870	548	111368	0.0	6.479	2.1	.06956	0.4	6.479	2.1	.06956	0.4	1.480	2.1	.1543	2.1	.99	925	18	915	7
1235-08bx	m	113	34	3381	0.6	6.648	2.1	.07567	1.0	6.648	2.1	.07567	1.0	1.570	2.3	.1504	2.1	.91	903	18	1086	19
1235-09a	c	200	110	89908	0.0	6.552	2.1	.06984	0.8	6.552	2.1	.06984	0.8	1.470	2.2	.1526	2.1	.94	916	18	924	16
1235-09b	m	129	38	11567	0.2	6.464	2.1	.07094	0.9	6.464	2.1	.07094	0.9	1.513	2.3	.1547	2.1	.92	927	18	956	18
1235-10a	c	598	314	115716	0.0	6.322	2.1	.06954	0.4	6.322	2.1	.06954	0.4	1.517	2.1	.1582	2.1	.98	947	18	915	9
1235-10b	m	122	38	20802	0.1	6.538	2.1	.07179	0.9	6.538	2.1	.07179	0.9	1.514	2.3	.1530	2.1	.92	918	18	980	19
64110, hypersthene quartz mangerite, Bjerkreim-Sokndal intrusion, Ljösvatn, E: 343600, y: 6481900 (7, 9)																						
1236-01a	c	130	66	63837	0.0	6.460	2.1	.06998	0.9	6.460	2.1	.06998	0.9	1.494	2.3	.1548	2.1	.92	928	18	928	18
1236-01c	m	246	75	74471	0.0	6.599	2.1	.06945	0.6	6.599	2.1	.06945	0.6	1.451	2.2	.1515	2.1	.96	910	18	912	13
1236-02a	c	1534	505	46037	0.0	6.586	2.1	.06979	0.3	6.586	2.1	.06979	0.3	1.461	2.1	.1518	2.1	.99	911	18	922	5
1236-02b	m	194	62	47770	0.0	6.552	2.1	.06992	0.7	6.552	2.1	.06992	0.7	1.471	2.2	.1526	2.1	.94	916	18	926	15
1236-03a	c	176	97	43686	0.0	6.631	2.1	.06988	1.1	6.631	2.1	.06988	1.1	1.453	2.4	.1508	2.1	.88	906	18	925	23
1236-03b	m	148	44	70202	0.0	6.347	2.1	.06968	1.0	6.347	2.1	.06968	1.0	1.514	2.3	.1576	2.1	.90	943	18	919	21
1236-04a	m	157	47	59437	0.0	6.487	2.1	.06988	1.0	6.487	2.1	.06988	1.0	1.485	2.3	.1542	2.1	.90	924	18	925	20
1236-05a	c	55	26	18999	0.1	6.799	2.1	.06978	1.4	6.799	2.1	.06978	1.4	1.415	2.5	.1471	2.1	.83	885	17	922	29
1236-05b	m	315	105	46622	0.0	6.840	2.1	.07069	0.6	6.840	2.1	.07069	0.6	1.425	2.2	.1462	2.1	.96	880	17	948	12
1236-06a	c	1700	361	32550	0.1	6.610	2.1	.06959	0.3	6.610	2.1	.06959	0.3	1.452	2.1	.1513	2.1	.99	908	18	916	6
1236-06b	m	533	145	125190	0.0	6.556	2.1	.06954	0.5	6.556	2.1	.06954	0.5	1.463	2.1	.1525	2.1	.98	915	18	915	9
1236-07a	c	85	34	7372	0.3	6.309	2.1	.07121	1.2	6.309	2.1	.07121	1.2	1.556	2.4	.1585	2.1	.88	948	19	963	23
1236-07b	m	202	65	65792	0.0	6.485	2.1	.07022	0.7	6.485	2.1	.07022	0.7	1.493	2.2	.1542	2.1	.94	924	18	935	15
1236-08a	c	198	98	97095	0.0	6.459	2.1	.06944	0.7	6.459	2.1	.06944	0.7	1.482	2.2	.1548	2.1	.94	928	18	912	15
1236-09a	c	232	141	35745	0.1	6.575	2.1	.06968	0.7	6.575	2.1	.06968	0.7	1.461	2.2	.1521	2.1	.95	913	18	919	14
1236-10a	c	184	72	14461	0.1	6.581	2.1	.06978	0.8	6.581	2.1	.06978	0.8	1.462	2.2	.1519	2.1	.93	912	18	922	17
1236-11a	c	128	43	34196	0.1	6.547	2.1	.07058	0.9	6.547	2.1	.07058	0.9	1.486	2.3	.1527	2.1	.92	916	18	945	18
1236-11b	m	269	86	57118	0.0	6.581	2.1	.06975	0.7	6.581	2.1	.06975	0.7	1.461	2.2	.1520	2.1	.95	912	18	921	15
64104, jotunite, Lomland dyke, Klungland, E: 359100, y: 6460300 (7, 9)																						
1237-01a	c	22	12	7823	0.2	6.544	2.1	.07009	2.2	6.544	2.1	.07009	2.2	1.477	3.0	.1528	2.1	.69	917	18	931	45
1237-01b	m	15	6	4359	0.4	6.418	2.1	.07133	2.7	6.418	2.1	.07133	2.7	1.532	3.4	.1558	2.1	.62	933	18	967	53
1237-02a	c	29	10	>1e6	0.0	6.596	2.1	.07115	1.9	6.596	2.1	.07115	1.9	1.487	2.9	.1516	2.1	.74	910	18	962	39
1237-03ax	c	18	10	22044	0.1	6.944	2.1	.07162	3.2	6.944	2.1	.07162	3.2	1.422	3.8	.1440	2.1	.55	867	17	975	63

Table 4 (*continued*)

Id	Z	U	Th	206Pb	f	238U	±	207Pb	±	238U	±	207Pb	±	207Pb	±	206Pb	±	Co	206Pb	±	207Pb	±
				204Pb		206Pb	1σ	206Pb	1σ	206Pb	1σ	206Pb	1σ	235U	1σ	238U	1σ		238U	1σ	206Pb	1σ
					%		%		%		%		%		%		%		Ma		Ma	
1	2	ppm	ppm		3	4		4		5		5		5		5		6	5		5	
1237-03b	m	12	5	2243	0.8	6.486	2.1	.07419	3.0	6.486	2.1	.07419	3.0	1.577	3.7	.1542	2.1	.57	924	18	1047	60
1237-04a	m	27	9	9645	0.2	6.571	2.1	.07143	2.0	6.571	2.1	.07143	2.0	1.499	2.9	.1522	2.1	.72	913	18	970	40
1237-05a	c	87	66	15013	0.1	6.650	2.1	.07036	1.2	6.650	2.1	.07036	1.2	1.459	2.4	.1504	2.1	.87	903	18	939	24
1237-05b	m	13	5	2843	0.7	6.722	2.1	.06831	2.9	6.722	2.1	.06831	2.9	1.401	3.6	.1488	2.1	.59	894	18	878	59
1237-06a	c	28	14	7931	0.2	6.596	2.1	.07333	1.9	6.596	2.1	.07333	1.9	1.533	2.9	.1516	2.1	.73	910	18	1023	39
1237-06b	m	11	4	3998	0.5	6.426	2.1	.06952	3.1	6.426	2.1	.06952	3.1	1.492	3.7	.1556	2.1	.56	932	18	914	62
1237-07a	c	14	6	3302	0.6	6.572	2.1	.07184	3.1	6.572	2.1	.07184	3.1	1.507	3.7	.1522	2.1	.56	913	18	981	62
1237-07b	m	12	5	5317	0.4	6.436	2.1	.07316	3.0	6.436	2.1	.07316	3.0	1.567	3.7	.1554	2.1	.57	931	18	1018	60
1238-01a	c	13	5	1565	1.2	6.428	2.1	.07497	3.1	6.428	2.1	.07497	3.1	1.608	3.7	.1556	2.1	.56	932	18	1068	61
1238-02a	c	17	8	3026	0.6	6.370	2.1	.07052	2.3	6.370	2.1	.07052	2.3	1.527	3.1	.1570	2.1	.66	940	18	944	47
1238-03a	c	17	9	1574	1.2	6.454	2.2	.07311	3.4	6.454	2.2	.07311	3.4	1.562	4.1	.1549	2.2	.54	929	19	1017	68
1238-03b	m	18	7	1460	1.3	6.519	2.1	.07997	2.3	6.519	2.1	.07997	2.3	1.691	3.1	.1534	2.1	.67	920	18	1196	45
1238-04a	c	14	10	2910	0.6	6.505	2.1	.07573	2.6	6.505	2.1	.07573	2.6	1.605	3.3	.1537	2.1	.63	922	18	1088	51
1238-05a	c	13	6	2229	0.8	6.637	2.1	.07741	3.3	6.637	2.1	.07741	3.3	1.608	3.9	.1507	2.1	.54	905	18	1132	64
1238-06a	c	19	9	2606	0.7	6.503	2.1	.07629	2.8	6.503	2.1	.07629	2.8	1.617	3.5	.1538	2.1	.60	922	18	1103	54

1: Analysis identifier, x: not selected for age calculation.
2: c: center of crystal, m: margin.
3: Proportion of total ^{206}Pb made of common ^{206}Pb.
4: Ratios uncorrected for common Pb.
5: Ratios and ages corrected for common Pb using ^{204}Pb signal, if the signal is above background.
6: Correlation of errors.
7: UTM(WGS84) coordinates, zone 32.
8: SHRIMP II data, Curtin University of Technology, Perth.
9: CAMECA, 1270 data, NORDSIM, Stockholm.

microscope (Fig. 3) prior to U–Pb analysis. For one sample (SV11), the measurements were carried out on the Perth Consortium SHRIMP-II ion microprobe at Curtin University of Technology (Perth, Australia). Each analysis consisted of 6 scans through the mass range; the primary beam was about 20 μm in diameter and 4 nA in intensity. The data were reduced in a manner similar to that described by Williams (1998) and references therein, using the SQUID Excel Macro of Ludwig (2000). The Pb/U ratios were normalized relative to a value of 0.090586 for the ^{206}Pb/^{238}U ratio of the BR266 reference zircon (Sri Lankan gem zircon), equivalent to an age of 559 Ma (Stern, 2001). For the five remaining samples, measurements were performed with a CAMECA 1270 ion microprobe at the NORDSIM Laboratory (Stockholm, Sweden) with a primary beam of ca. 20 μm in diameter, using the 91500 Geostandard reference zircon with an age of 1065 Ma (Wiedenbeck et al., 1995). Analytical protocols and data reduction follow Whitehouse et al. (1999) and Whitehouse and Kamber (2005). Data are reported in Table 4 and in inverse Terra–Wasserburg concordia diagrams in Fig. 3. Age calculations were performed using the Isoplot 3 Excel macro (Ludwig, 2003). In Fig. 3, analyses are plotted with a one sigma error ellipse, but all age calculations are reported at the two sigma level. The analyses are corrected for common Pb using the ^{204}Pb signal, if this signal is above background. For the two samples characterized by zircon with low U content (66125, U<77 ppm; 64104, U<87 ppm), a ^{207}Pb common Pb correction (projection of the uncorrected analysis on the concordia curve in the inverse concordia diagram from a common Pb composition) is regarded as more appropriate (Fig. 3).

4. Comparison between key Sveconorwegian magmatic suites

In the following, we will compare the geological setting, petrography and geochemistry of the Feda, HBG and AMC suites to setup their mutual links.

4.1. Geology

4.1.1. The Feda suite

The Feda suite is comprised of most of the augen gneiss bodies outcropping in the Rogaland–Vest Agder sector (Bingen, 1989; Bingen et al., 1993; Figs. 1B and 2A). The augen gneiss bodies are conformable with regional structural trends and show locally, in their center, less deformed rock volumes with preserved porphyritic igneous textures. They are interpreted as pre- to syn-tectonic amphibole–biotite granodioritic to granitic plutons rich in K-feldspar phenocrysts and defining an "orogenic" high-K calc-alkaline trend (Bingen and van Breemen, 1998a; Bingen et al., 2008). Uncommon gabbroic enclaves display lobate contacts with the enclosing granodiorites. Two types of enclaves are recognized: *K-rich enclaves*, which are similar in composition to lamprophyric magmas and can be included in Group III ultrapotassic rocks of Foley (1992); and *amphibole-rich enclaves* with a calc-alkaline affinity. Samples BB17a, BB120b and BB82b analyzed in this study belong to this last category. Given that these lobate enclaves are mingled in the main granodioritic magma, they represent penecontemporaneous mafic magmas. Rocks of the Feda suite show LILE enrichment together with rather low Sr_i, positive ε_{Nd} and low Pb isotopic ratios (at 1.05 Ga: $Sr_i = 0.7035$, $\varepsilon_{Nd} = +0.6$, $(^{206}Pb/^{204}Pb)_i = 17.07$, $(^{207}Pb/^{204}Pb)_i = 15.46$ (average of initial isotopic values of 11 K-feldspar phenocrysts: Bingen et al., 1993)). The main granodioritic to granitic Feda trend has been interpreted as being due to fractional crystallization, without high level contamination by the surrounding gneisses (Bingen et al., 1993).

4.1.2. The HBG suite

The spatial distribution of the post-collisional granitoids is not random. They are concentrated along two major crustal boundaries, namely the Mandal–Ustaoset fault/shear zone and the Østfold–Marstrand boundary zone (Fig. 1A). Andersen (1997), Andersen et al. (2001) and Andersen et al. (2002a) undertook a comprehensive isotopic study (Sr, Nd, Pb, Hf) of these granitoids distinguishing three groups of granitoids based on their Sr contents and Sr and Nd isotopic compositions. The group 1 granites ("normal Sr concentration granites") have more than 150 ppm Sr, $^{87}Rb/^{86}Sr < 5$, $^{87}Sr/^{86}Sr_{0.93Ga} < 0.710$ and $\varepsilon Nd < 0$. The group 2 granites have less than 150 ppm Sr, $^{87}Rb/^{86}Sr > 5$, $^{87}Sr/^{86}Sr_{0.93Ga} > 0.710$ and $\varepsilon Nd < 0$. Group 3 is comprised of one peculiar granite (the Tovdal granitoid: Fig. 1) characterized by low $^{87}Sr/^{86}Sr_{0.93Ga}$ (<0.710) and high εNd (>0). These authors showed that granites of group 1 are the most abundant and ubiquitous in south Norway. They further suggested that

group 1 isotopic compositions are consistent with mixing between a depleted-mantle component and two components having an extended crustal history. Group 2 granites are low in Sr and restricted to north-central Telemark. Recent geochronological data (Andersen et al., 2002a, 2007a) have shown that, with the exception of the Bessefjellet (940 ± 19 Ma: Andersen et al., 2002a) and Torsdalsfjell (990 ± 14 Ma: Andersen et al., 2007a) intrusions, group 2 granitoids range in age from 1.023 Ga to 1.168 Ga and are thus older than both the Sveconorwegian regional metamorphism and the HBG suite.

Vander Auwera et al. (2003) performed a geochemical study of a selection of granitoids (Kleivan, Holum, Svöfjell, Rustfjellet, Valle, Bessefjellet, Verhuskjerringi: Fig. 1B) occurring along the Mandal–Ustaoset fault and shear zone. These granitoids fall in the "normal Sr concentration group" (group 1) defined by Andersen et al. (2001) except Bessefjellet which belongs to group 2. The selected granitoids have similar field and petrographic characteristics, as well as similar major and trace element compositions (Vander Auwera et al., 2003). Their mafic mineralogy is dominated by hornblende and biotite with clinopyroxene occurring only as relic cores in amphibole. The other minerals are plagioclase, K-feldspar, quartz, apatite, zircon, ilmenite and magnetite. Titanite and fluorite have also been observed. They have been referred to as the HBG (Hornblende and Biotite Granitoids) suite by Vander Auwera et al. (2003). The granitoids are ferroan (Frost et al., 2001), mostly metaluminous and display elevated concentrations of Ga and incompatible elements, typical of A-type granites (Whalen et al., 1987). Bogaerts et al. (2003a) documented their rapakivi-like composition in a detailed petrological study of the Lyngdal granodiorite. On the basis of experimental data acquired on two different samples (quartz monzodiorite, granodiorite) of the Lyngdal intrusion, Bogaerts et al. (2006) concluded that its parent magma, quartz monzodioritic in composition, was emplaced in the upper crust (0.2–0.4 GPa) and was relatively wet (5–6 wt.% H_2O) and oxidized (oxygen fugacity at NNO to NNO + 1). Finally, thermo-rheological modeling performed on the Lyngdal granodiorite (HBG suite) suggests that final emplacement of the magma took place at the brittle/ductile transition of the crust which was shallow in this area due to a high heat flow of 100 mW/m^2 (Bogaerts et al., 2003b).

In the HBG suite, mafic components were recognized as lobate mafic microgranular enclaves (MME) (Barbarin and Didier, 1992) that are locally mingled in the more evolved compositions (monzodiorites, granodiorites) or as small intrusions spatially associated with the granitoids. Vander Auwera et al. (2008) used these mafic facies to show that the monzodioritic parent magma of the granitoids could be produced either by: a) partial melting of a mafic lower crust equivalent in composition to the observed mafic facies, or b) by fractional crystallization of this mafic component, although partial melting is better predicted by geochemical modeling. Either process produces abundant mafic rocks either as cumulates or restites. However, as such rocks are not observed at the present level of exposure, this differentiation step probably occurred in the lower crust. As discussed by Vander Auwera et al. (2008), the mainly leucogranitic composition of the Rustfjellet intrusion (Vander Auwera et al., 2003) is close to the composition of minimum melts, suggesting that it may result from partial melting of a more acidic crustal source.

The conclusions presented by Bogaerts et al. (2003a), Vander Auwera et al. (2003), Bogaerts et al. (2006), Vander Auwera et al. (2008) and in the present paper concern the HBG suite outcropping along the Mandal–Ustaoset Line. As these rocks have similar major and trace element concentrations (e.g. Pedersen and Konnerup-Madsen, 2000) and Sr, Nd and Pb isotopic compositions as the Telemark granitoids (Andersen et al., 2001), it is possible that these conclusions can be extended to all group 1 granitoids.

4.1.3. The AMC suite

The Anorthosite–Mangerite–Charnockite (AMC) suite of Rogaland (Figs. 1B and 2B), is composed of three massif-type anorthosites (Egersund–Ogna, Håland–Helleren, and Åna–Sira), a large layered intrusion (Bjerkreim–Sokndal), two smaller leuconoritic bodies (Hidra, Garsaknatt) and a small volume of mafic rocks ranging in composition from high-Al gabbros to jotunites (hypersthene-bearing monzodiorites). Few high-Al gabbros, mostly occurring as dykes crosscutting the Egersund Ogna anorthosite, have been recognized (Charlier et al., 2010). The jotunites display a range of composition and are more abundant, especially the evolved jotunites sensu Vander Auwera et al. (1998). The jotunites occur as small intrusions, chilled margins or dykes (Duchesne, 1987; Duchesne and Korneliussen, 2003). Among these dykes, the Tellnes dyke, that crosscuts the Åna-Sira anorthosite, displays a complete differentiation trend from jotunites to quartz mangerites (Wilmart et al., 1989). The rocks of the AMC suite are composed of plagioclase (antiperthitic in the evolved compositions), orthopyroxene, clinopyroxene, ilmenite, magnetite, apatite, with K-feldspar (usually perthitic to mesoperthitic), zircon and quartz only in the differentiated facies. The AMC suite is characterized by the predominance of orthopyroxene among the ferromagnesian minerals (charnockitic suite) and the very low abundance of amphibole and biotite. Amphibole is lacking in the jotunites and mangerites and has only been observed locally in the quartz mangerites to charnockites (Dekker, 1978). In the upper part of Bjerkreim–Sokndal and in the Apophysis, a foliated sheet-like body extending southwards from the margin of the Bjerkreim–Sokndal intrusion (Fig. 2B), amphibole occurs as poikilitic grains in dm-sized patches of coarse-grained mangerites and quartz mangerites and as rims surrounding the Fe–Ti oxides (Duchesne and Wilmart, 1997; Bolle and Duchesne, 2007).

The Bjerkreim–Sokndal layered intrusion represents an important member of the Rogaland AMC suite (Fig. 2B). Its lower part is made up of a thick layered series subdivided in several megacyclic units (Wilson et al., 1996). Its upper part comprises more massive acidic rocks (mangerites, quartz mangerites, charnockites) that extend southwards into the Apophysis. Two different trends have been recognized in the upper acidic part of Bjerkreim–Sokndal: a two pyroxene-amphibole trend (PXT) that grades from two-pyroxene quartz mangerites to amphibole and two-pyroxene charnockites, and an olivine trend (OLT) that is comprised of olivine-bearing quartz mangerites and charnockites. The OLT has been interpreted as being genetically linked with the underlying cumulates of the Bjerkreim–Sokndal intrusion, whereas the PXT would be derived from a jotunitic melt which mingled with the resident magma (Duchesne and Wilmart, 1997). The Apophysis appears as a composite igneous body comprising coeval mafic to felsic magmas (Bolle and Duchesne, 2007). The differentiation trend of the felsic magmas in the Apophysis is slightly different, mineralogically and geochemically, than those (PXT, OLT) recognized in the upper part of Bjerkreim–Sokndal, suggesting that it preserves evidence for the existence of a third trend (APT) (Bolle and Duchesne, 2007).

Recent geochemical data on the composition of orthopyroxene and plagioclase megacrysts from the Egersund–Ogna anorthosite support the hypothesis that more than one parental melt composition is necessary to account for the petrogenesis of the whole AMC suite (Duchesne and Demaiffe, 1978; Duchesne et al., 1985a; Duchesne and Hertogen, 1988; Vander Auwera and Longhi, 1994; Charlier et al., 2010). As jotunitic chilled margins were sampled around the Hidra leuconoritic body (Duchesne et al., 1974; Demaiffe and Hertogen, 1981) and the Bjerkreim–Sokndal layered intrusion (Duchesne and Hertogen, 1988; Robins et al., 1997), jotunites were considered as possible parental melts for these intrusions in agreement with experimental data later acquired on a primitive (high Mg#) jotunite (TJ) (Vander Auwera and Longhi, 1994). However, based on the high Cr content measured in the high-Al orthopyroxene megacrysts of the Egersund–Ogna anorthosite, a more basaltic parental melt was proposed for this intrusion (Duchesne et al., 1985a; Duchesne and Maquil, 1987). Duchesne and Maquil (1987) also indicated that the plagioclase megacrysts from the Egersund–Ogna anorthosite display

cryptic geographical variation: high-Sr (720–1090 ppm) andesine in the center and low-Sr (320–620 ppm) labradorite in the margin (Charlier et al., 2010). Based on experimental data on a high-Al gabbroic composition (HLCA) (Fram and Longhi, 1992) and a primitive jotunite (TJ) (Vander Auwera and Longhi, 1994) and on the increasing partition coefficient of Cr in orthopyroxene with pressure (Vander Auwera et al., 2000), it was later suggested that the central part (andesine anorthosite) of the Egersund–Ogna anorthosite could have crystallized from a jotunitic parent magma slightly more magnesian and more anorthitic than the experimentally studied TJ composition (Longhi et al., 1999). This hypothesis was further tested by Charlier et al. (2010). These authors concluded that the high Mg # (55–79) of the orthopyroxene from the center and the margin of the Egersund–Ogna anorthosite cannot be produced from a primitive jotunite more magnesian than TJ. They thus proposed that the central and marginal anorthosites from this intrusion both had a high-alumina basaltic parental melt but with different CaO, Sr, Mn and Cr contents. A range of parental melt composition, from high-Al basalts to primitive jotunites, appears thus necessary to account for the petrogenesis of the AMC suite.

Experimental data on the liquidus equilibria of a high-Al basalt (HLCA) and a primitive jotunite (TJ) indicate that between 10 and 13 kbar, the pressure conditions necessary to produce the characteristic high-Al orthopyroxene megacrysts (Longhi et al., 1993), these compositions straddle the thermal divide on the plagioclase + pyroxene liquidus surface (Longhi et al., 1999). This observation requires that these melts were produced by partial melting of a gabbronoritic lower crustal source (Longhi et al., 1999). Plausible compositions for this lower crustal source have been discussed in detail by Longhi et al. (1999) and Longhi (2005). Average compositions of a lower granulitic crust (Rudnick and Fountain, 1995) are possible, but the bulk composition of the Stillwater Banded Zone appears as a better candidate given its higher Mg# (Longhi et al., 1999; Longhi, 2005). Also, as mentioned by Longhi et al. (1999) and Longhi (2005), the upper part of layered mafic intrusions usually contains cumulates with higher concentrations of K, Ti and P which make them possible sources for jotunitic magmas. These authors further proposed that foundering of gravitationally unstable mafic to ultramafic masses in the upper mantle (Arndt and Goldstein, 1989) might induce their partial melting. Other possible scenarios for melting the lower crust have been proposed: magmatic heating from below, crustal thickening, thrusting of tongues of lower crust into the mantle (Duchesne et al., 1999; Longhi et al., 1999). This latter process has been discussed in more detail by Duchesne et al. (1999). Based on the work of Andersson et al. (1996) who interpreted large Moho offsets in deep seismic profiles as resulting from Sveconorwegian crustal underthrusting, these authors suggested that underthrust crustal tongues of mafic lower crust were heated to their solidus to produce the parent magma of the AMC suite because of thermal relaxation of several tens of million years together with asthenospheric uprise due to delamination along the shear zone (see also Lundmark and Corfu, 2008). Duchesne et al. (1999) also emphasized that the uprise of the anorthositic crystal mushes and magmas were chanelled by the presence of major lithospheric structures as is observed in other anorthositic provinces (e.g. Emslie et al., 1994; Scoates and Chamberlain, 1997; Wiszniewska et al., 2002). Finally, based on the occurrence of eclogite facies rocks in the Eastern segment, Brueckner (2009) recently proposed that during subduction of the Eastern Segment of Fennoscandia, the subducted continental crust separated in two parts: the shallower one was exhumed as the HP eclogites of the Eastern Segment whereas the lower part remained in the upper mantle. These authors proposed that this lower mafic part of the Eastern Segment crust subducted further to the west and was progressively metamorphosed to amphibolite, granulite and eclogite facies providing the source for the AMC and HBG suites. Brueckner (2009) indeed acknowledged that the source of the AMC suite is anhydrous whereas that of the HBG suite is hydrous as already discussed by Vander Auwera et al. (2008). Brueckner (2009) also suggested that the eclogitized crust detached and sunk into the mantle allowing upwelling of the asthenosphere and concomitant heating and partial melting of the stranded granulitic to amphibolitic subducted crust. This last model has some similarities with the crustal tongue model of Duchesne et al. (1999). However, the REE patterns of plausible AMC parent magmas display low $(La/Yb)_N$ precluding the presence of garnet in their source. Thus, partial melting must have occurred outside the stability field of garnet for these compositions, i.e. at a pressure $\leq$1.6 GPa (Fram and Longhi, 1992; Vander Auwera and Longhi, 1994). Consequently, given the large distance between the Eastern Segment and the AMC suite (about 380 km) together with the maximum 1.6 GPa pressure of partial melting, the inferred subduction angle is an implausible 3°.

Modeling of the differentiation of the primitive jotunitic magma using fine-grained samples (LLD) has shown that quartz mangerites can be produced by extreme differentiation of primitive jotunites. However, as pointed out by Duchesne et al. (1985b), Demaiffe et al. (1986) and Vander Auwera et al. (1998) it is also possible that part of the acidic rocks of the Rogaland Anorthosite Complex were produced directly by partial melting of the crust. Field and petrological evidence (low a_{H2O} in the granulite wall rock as evident from occurrence of osumilite (Holland et al., 1996), very few pegmatites and hydrous phases) indicate differentiation under nearly anhydrous conditions. Estimates of fO_2 range from FMQ + 1.3 to ca.FMQ-1 (Duchesne, 1972; Duchesne et al., 1989; Vander Auwera and Longhi, 1994; Duchesne et al., 2008), lower than or overlapping with the fO_2 range reported for the HBG suite (NNO to NNO + 1: Bogaerts et al., 2006).

Both magnetite and ilmenite have been observed in the HBG and AMC suites, but the magnetite/ilmenite ratio appears to be higher in the HBG suite. This observation is supported by published data on the magnetic susceptibility of bulk samples representative of liquid compositions and ranging in composition from 57 to 74% SiO_2. As shown on Fig. 4, there is some overlap in the range of magnetic susceptibilities obtained in the two suites but in the AMC suite, the bulk magnetic susceptibility of most samples ranges between 0 and 30 mSI compared to 40 and 90 mSI in the HBG suite. This is corroborated by recent results of Brown and McEnroe (2008) who showed that in the three massif type anorthosites of the AMC suite, namely Egersund–Ogna, Åna–Sira and Haland–Helleren (Fig. 2B), magnetite is rare or only locally observed whereas hemo-ilmenite is a common accessory phase, the magnetic susceptibility being correlated with the proportion of magnetite present in their samples. It has been experimentally shown that the relative stability of the Fe–Ti oxides is strongly controlled by oxygen fugacity and that a higher fO_2 increases the stability field of magnetite (Buddington and Lindsley, 1964; Frost, 1991; Snyder et al., 1993; Toplis and Carroll, 1995). However, crystallization of ilmenite is enhanced by a high TiO_2 content in the magma (Toplis and Carroll, 1995). As the AMC and HBG suites have similar TiO_2 contents, the higher proportion of magnetite in the HBG suite probably reflects a higher fO_2 during crystallization. Bogaerts et al. (2006), using experimental data, proposed an fO_2 of NNO to NNO + 1 during the differentiation of the Lyngdal intrusion whereas for the AMC suite, fO_2 between FMQ-1 and NNO have been proposed (Duchesne, 1972; Vander Auwera and Longhi, 1994; Brown and McEnroe, 2008).

4.2. Geochronology

Four granodioritic to granitic augen gneiss bodies of the Feda suite, the 'orogenic' intrusions predating the emplacement of the post-collisional suites, distributed over 100 km across regional structural trends and across the orthopyroxene isograd yield a very consistent intrusion age of 1051 +2/–8 to 1049 +2/–8 Ma (Bingen and van Breemen, 1998a). Metamorphic monazite in clinopyroxene and/or orthopyroxene-bearing samples ranges mainly between 1024 and

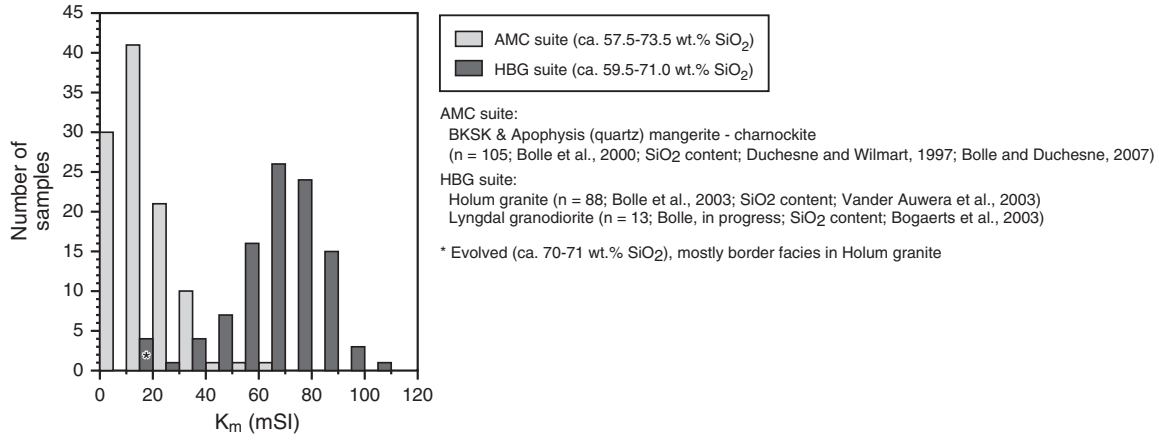

Fig. 4. Bulk magnetic susceptibilities (K_m (mSI) $= (K_1 + K_2 + K_3)/3$, $K_1 \geq K_2 \geq K_3$ are the three principal axes of the ellipsoid describing anisotropy of the magnetic susceptibility in a low magnetic field) of the AMC and HBG suites.
Data from Bolle et al. (2000), Bolle et al. (2003b) and Bolle and Duchesne (2007).

925 Ma recording M1 and M2 high-grade metamorphism respectively (Bingen and van Breemen, 1998b). The Fennefoss augen gneiss in the Telemark sector is distinctly younger than the Feda suite as it intruded at 1035 ± 3 Ma (Bingen and van Breemen, 1998a) and it is also geochemically distinct.

The oldest dated but arguably post-collisional pluton is the Grimstad granite in the Bamble terrane. It has an age of 989 ± 9 Ma (Kullerud and Machado, 1991). In the Telemarkia terrane, post-collisional plutons forming the HBG suite range in age between 970 and 932 Ma. The most reliably dated plutons are the Vrådal pluton in Telemark with two overlapping ages at 970 ± 6 and 964 ± 18 Ma (Andersen et al., 2007a), the Holum granite on the western side of the Mandal–Ustaoset fault and shear zone in the Rogaland–Vest Agder sector at 957 ± 7 Ma (Bingen et al., 2006), the Tovdal pluton in Telemark at 940 ± 10 (Andersen et al., 2002a) and the Verhuskjerringi granite at 932 ± 4 Ma (Andersen et al., 2007a).

A new age determination is reported here for the Svöfjell pluton which is one of the largest HBG plutons exposed along the Mandal–Ustaoset fault and shear zone. In granite sample SV11, seven elongate prismatic zircons with oscillatory-growth zoning were analyzed. Data are nearly concordant within error limits. Data corrected for common Pb yield a concordia age of 942 ± 10 Ma (MSWD of concordance + equivalence = 2.2, Th/U = 0.53, Fig. 3A). No inherited zircon cores were detected. The 942 ± 10 Ma estimate is interpreted as the crystallization age of the Svöfjell pluton, in the range known for the HBG suite.

The age of crystallization of the three large massif type anorthosite bodies in the AMC suite was measured by Schärer et al. (1996) using zircon included in orthopyroxene megacryst aggregates. Three equivalent ages of 932 ± 3, 932 ± 3 and 929 ± 2 Ma were derived for the Håland–Helleren, Åna–Sira and Egersund–Ogna anorthosites respectively. A quartz-mangerite from the Tellnes dyke crosscutting the Åna–Sira anorthosite gives an equivalent age of 931 ± 5 Ma while the associated Tellnes ilmenite norite yields a significantly younger age of 920 ± 3 Ma. To improve data coverage, new data were collected in five zircon-bearing units of the AMC suite (Fig. 2).

Sample 7234 is a fine-grained primitive jotunite (monzonorite) from the margin of the small Hidra leuconorite pluton, approximating the composition of the parental magma of this pluton (Duchesne et al., 1974; Demaiffe and Hertogen, 1981; Duchesne et al., 1989). The sample contains xenomorphic non-luminescent high-U zircon, showing only weak internal zoning. Five analyses in four zircons, corrected for common Pb, yield a concordia age of 932 ± 9 Ma (Th/U = 0.48; Fig. 3B). This age is interpreted to record the crystallization age of the rock and is equivalent to the pioneering U–Pb age of 931 ± 10 Ma derived by Pasteels et al. (1979) from a charnockitic dyke cutting the Hidra pluton.

Sample 66125 is a quartz jotunite (monzonorite) from the Eia–Rekefjord intrusion, which is an elongate jotunitic to mangeritic body at the interface between the Bjerkreim–Sokndal intrusion and the Håland–Helleren anorthosite (Duchesne et al., 1974). The Eia–Rekefjord intrusion is younger than the Håland–Helleren anorthosite, since dykes interpreted as emanating from this intrusion crosscut the anorthosite. Zircons show a core–rim structure, with a generally non-luminescent core and a luminescent low-U rim. The rim is coarse, xenomorphic and locally hat-shaped (Fig. 3C), suggesting an overgrowth process by subsolidus redistribution of Zr originally hosted in ilmenite, as described in Bingen et al. (2001), Charlier et al. (2007) and Morisset and Scoates (2008). Six analyses in six zircon cores are concordant to slightly discordant. They have an average Th/U ratio of 1.02 characteristic of magmatic crystallization. They yield a ^{207}Pb corrected $^{206}Pb/^{238}U$ intercept age of 932 ± 8 Ma (Fig. 3C) equivalent to a weighted mean ^{204}Pb corrected $^{206}Pb/^{238}U$ age of 930 ± 8 Ma. These ages are equal to the age of 932 ± 3 Ma for the adjacent Håland–Helleren anorthosite (Schärer et al., 1996).

Sample 66261 is a fayalite-bearing quartz mangerite from the upper part of the Bjerkreim–Sokndal intrusion. It represents the olivine trend (OLT) genetically linked with the underlying cumulates and hybridized with new magma (Duchesne and Wilmart, 1997). Zircons of this sample are commonly characterized by a high-U core surrounded by an oscillatory-zoned mantle (Duchesne et al., 1987a). Nineteen analyses were performed in 10 zircons. All but two analyses are concordant and contain background level common Pb. Five non-luminescent high-U cores have U concentrations higher than 500 ppm (average U = 1020 ppm and Th/U = 0.48). They yield a concordia age of 931 ± 7 Ma (MSWD = 1.6, Fig. 3D). Other cores and mantles have U concentrations lower than 300 ppm (average U = 150 ppm and Th/U = 0.35), and yield a significantly younger, though overlapping, concordia age of 919 ± 8 Ma (MSWD = 1.12, Fig. 3D). The data suggest that the high-U cores crystallized at 931 ± 7 Ma in the residual magma left after crystallization of the cumulates, whereas the rims crystallized at 919 ± 8 Ma, only after mixing of this resident magma with a new batch of acidic magma. The age of 931 ± 7 Ma represents the best available estimate for the crystallization of the Bjerkreim–Sokndal layered series.

Sample 64110 is a quartz mangerite also from the upper part of the Bjerkreim–Sokndal intrusion. It belongs to the two pyroxenes–amphibole trend (PXT), presumably derived from a jotunitic melt mingled with the resident magma (Duchesne and Wilmart, 1997).

Zircons of this sample are also commonly characterized by a non-luminescent high-U core surrounded by an oscillatory-zoned mantle (Duchesne et al., 1987a). Eighteen analyses were performed in 11 zircons. The analyses are concordant and contain background level common Pb. Three analyses of high-U cores (U >500 ppm) yield a concordia age of 918 ± 8 Ma, equivalent to the concordia age of 922 ± 7 Ma for 15 analyses of mantles and cores moderately rich in U (U < 320 ppm). The pooled dataset (18 analyses) yield a concordia age of 920 ± 6 Ma (MSWD = 0.83), giving the best estimate for crystallization of this rock (Fig. 3E). This result supports the interpretation that part of the upper part of the Bjerkreim–Sokndal intrusion results from the crystallization of a batch of acidic magma distinctly younger (ca. 920 Ma) than the magmas that generated the cumulates (ca. 931 Ma).

Sample 64104 is a jotunite (monzonorite) from the Lomland monzonoritic dyke. This dyke is more than 20 km long and crosscuts the Egersund–Ogna anorthosite and the layered series of the Bjerkreim–Sokndal intrusion (Duchesne et al., 1985b). It shows a continuous variation from norite to jotunite. The sample contains luminescent, low-U, oscillatory zoned zircon commonly overgrown by a rim. Nineteen analyses were performed in 13 zircon crystals, including cores and rims. The analyses have U concentrations lower than 87 ppm and a Th/U ratio of 0.47. All but one analysis yield a well grouped ^{207}Pb corrected ^{206}Pb/^{238}U intercept age of 916 ± 9 Ma (MSWD = 0.47; Fig. 3F) equivalent to a weighted mean ^{204}Pb corrected ^{206}Pb/^{238}U age of 919 ± 8 Ma. The age of 916 ± 9 Ma is regarded as the best estimate for the crystallization of the dyke. It is equivalent to the age of the Tellnes ilmenite norite (920 ± 3 Ma), and provides independent evidence for a generation of jotunitic magma at around 920 Ma emplaced in crosscutting structures.

The data by Schärer et al. (1996) bracket the entire AMC suite within a 12 million year interval. The new data confirm this time bracket and show that the main magmatic pulse took place at 933–929 Ma, leading to formation of the massif-type anorthosites, satellite leuconorite plutons (Hidra pluton), the Bjerkreim–Sokndal layered intrusion and a number of minor occurrences of monzonorite (Eia–Rekefjord intrusion, Tellnes dyke). A second minor magmatic pulse took place at 920–916 Ma and corresponds to the intrusion of jotunitic magmas and related acidic melts in dykes (Tellnes ilmenite norite, Lomland dyke) and at the roof of the Bjerkreim–Sokndal intrusion during the final stage of sagging of the lower part of the intrusion (Bolle et al., 2000), resulting in crystallization of part of the mangerite–charnockite sequence at the top of this intrusion. The data underscore the composite nature of the Bjerkreim–Sokndal intrusion.

4.3. Geochemistry

The geochemistries of the AMC and HBG suites are compared using available databases. For the AMC suite, the following data have been employed: the Apophysis of the Bjerkreim–Sokndal layered intrusion (APT) (Bolle and Duchesne, 2007), the olivine- (OLT) and pyroxene- (PXT) bearing trends observed in the upper part of Bjerkreim–Sokndal (Duchesne and Wilmart, 1997), and finally the geochemical trend observed in the Tellnes dyke and in fine-grained samples (LLD) interpreted as representing the jotunite differentiation trend of the Rogaland AMC suite (Duchesne and Maquil, 1987; Wilmart et al., 1989; Robins et al., 1997; Vander Auwera et al., 1998; Bolle et al., 2003a). For the HBG suite, we have employed data from the granitoids emplaced in the Rogaland–Vest Agder sector close to the Mandal–Ustaoset fault and shear zone: Lyngdal, Tranevåg, the Red granite, Svöfjell, Valle, Rustfjellet, Holum and the gabbronorites (Demaiffe et al., 1990; Bogaerts et al., 2003a; Vander Auwera et al., 2003). The Tranevåg and Red granite bodies are located in the southernmost part of the Lyngdal intrusion and were recognized as separate bodies by Falkum et al. (1979) and Bogaerts et al. (2003a). Additional isotopic data are from Weis (1986), Bingen et al. (1993), Barling et al. (2000), Andersen et al. (2001), Dupont (2003) and Dupont et al. (2005). In the following, special attention will be given to the least differentiated compositions observed in both suites: the primitive jotunites and high-Al gabbros in the AMC suite, and the gabbronorites and mafic enclaves in the HBG suite.

4.3.1. Major and trace elements

According to the classification of Frost et al. (2001) and Frost and Frost (2008), both the AMC and HBG suites are ferroan (Fig. 5) and display geochemical features characteristics of an A-type signature, namely elevated contents of Ga (Ga/Al × 10,000 > 2.6) (not shown) and incompatible elements (Zr + Nb + Ce + Y > 350 ppm) (not shown). However, the AMC suite is alkalic to alkali-calcic whereas the HBG suite is frankly alkali-calcic, the AMC trend is higher in K_2O, $FeO_t/(FeO_t + MgO)$ and lower in CaO and MgO. The two trends overlap in TiO_2 (not shown) and to a lesser extent in P_2O_5. The mafic facies of both suites have overlapping major element compositions.

In order to take into account the position of one particular sample on the differentiation trend of each suite, we have compared each sample to the interpolated composition of a reference series at the same SiO_2 content as proposed by Liégeois et al. (1998). The reference series used here is the one proposed by Liégeois et al. (1998) i.e., the Yenchichi–Telabit series (Fig. 6). The normalized spider diagram shows that the AMC suite is lower in Rb, U, Th, Sr, CaO, Ce, Nd, Sm and higher in Zr, Hf and Fe_2O_{3t} than the HBG suite.

4.3.2. Sr, Nd and Pb isotopes

The Sr, Nd and Pb isotopic data clearly distinguish the HBG and AMC suites as shown on Fig. 7 where isotopic ratios have been calculated to the average emplacement age of the suites, respectively 0.93 Ga for the AMC suite and 0.95 Ga for the HBG suite. Data for the Feda suite are also shown.

In a $(^{206}Pb/^{204}Pb)_i$–$(^{207}Pb/^{204}Pb)_i$ diagram (Fig. 7), the least differentiated compositions of both suites have a similar range of ratios: AMC: $(^{207}Pb/^{204}Pb)_i = 15.48–15.54$ and $(^{206}Pb/^{204}Pb)_i = 17.28–17.66$; HBG: $(^{207}Pb/^{204}Pb)_i = 15.50–15.52$ and $(^{206}Pb/^{204}Pb)_i = 17.42–17.49$, but intermediate and acidic members of the HBG suite evolve toward low Pb isotopic ratios, whereas intermediate members of the AMC suite evolve to high Pb isotopic ratios.

The Sr and Nd isotopic (Fig. 7) composition of jotunitic and acidic members of the AMC suite have been studied in detail by Bolle et al. (2003a). These authors reported that the AMC suite starts from rather low $^{87}Sr/^{86}Sr_{0.93Ga}$ (0.7040–0.7060) and positive ε_{Ndt} (+4.7 to +1.2) in the primitive jotunites (the parent magmas of several members of the AMC suite) and evolves to high $^{87}Sr/^{86}Sr_{0.93Ga}$ (0.7070–0.7230) and lower to negative ε_{Ndt} (+1.4 to −1.7) in the felsic plutons. These authors interpreted this isotopic trend as contamination of the primitive jotunite magmas with a LILE-enriched crustal component and were able to reproduce this observed trend using a binary mixing model between these two components. The crustal contaminant, referred to as C1 by Bolle et al. (2003a), corresponds to an average isotopic composition of the Pre-Sveconorwegian rocks of southern Norway. It has been estimated using available coupled Sr and Nd isotopic data on the surrounding gneisses (Vander Auwera et al., 2003) and on amphibolite- to granulite-facies metasediments from the Bamble sector which are isotopically similar to the surrounding gneisses (Andersen et al., 1995; Knudsen et al., 1997) (Fig. 7). Available Pb isotopic data (see above) further indicate that this crustal contaminant must be characterized by high Pb isotopic ratios. The least differentiated compositions of the HBG suite, the gabbronorites, have low $^{87}Sr/^{86}Sr_{0.95Ga}$ (0.7047–0.7054) and positive ε_{Ndt} (+2.0 to +0.4) that overlap the compositions of the mafic facies of the AMC suite. However, contrarily to what is observed for the AMC suite, the intermediate and acidic members of the HBG suite evolve at nearly constant $^{87}Sr/^{86}Sr_{0.93Ga}$ (0.7042–0.7060) towards very negative ε_{Nd} (−0.9 to −5), implying a strikingly different crustal contaminant as discussed by Andersen et al. (1994), Knudsen et al. (1997), Bolle et al. (2003a), Vander Auwera et al. (2008) and referred to as contaminant C2 by Bolle et al. (2003a) and Vander Auwera et al. (2008). This crustal

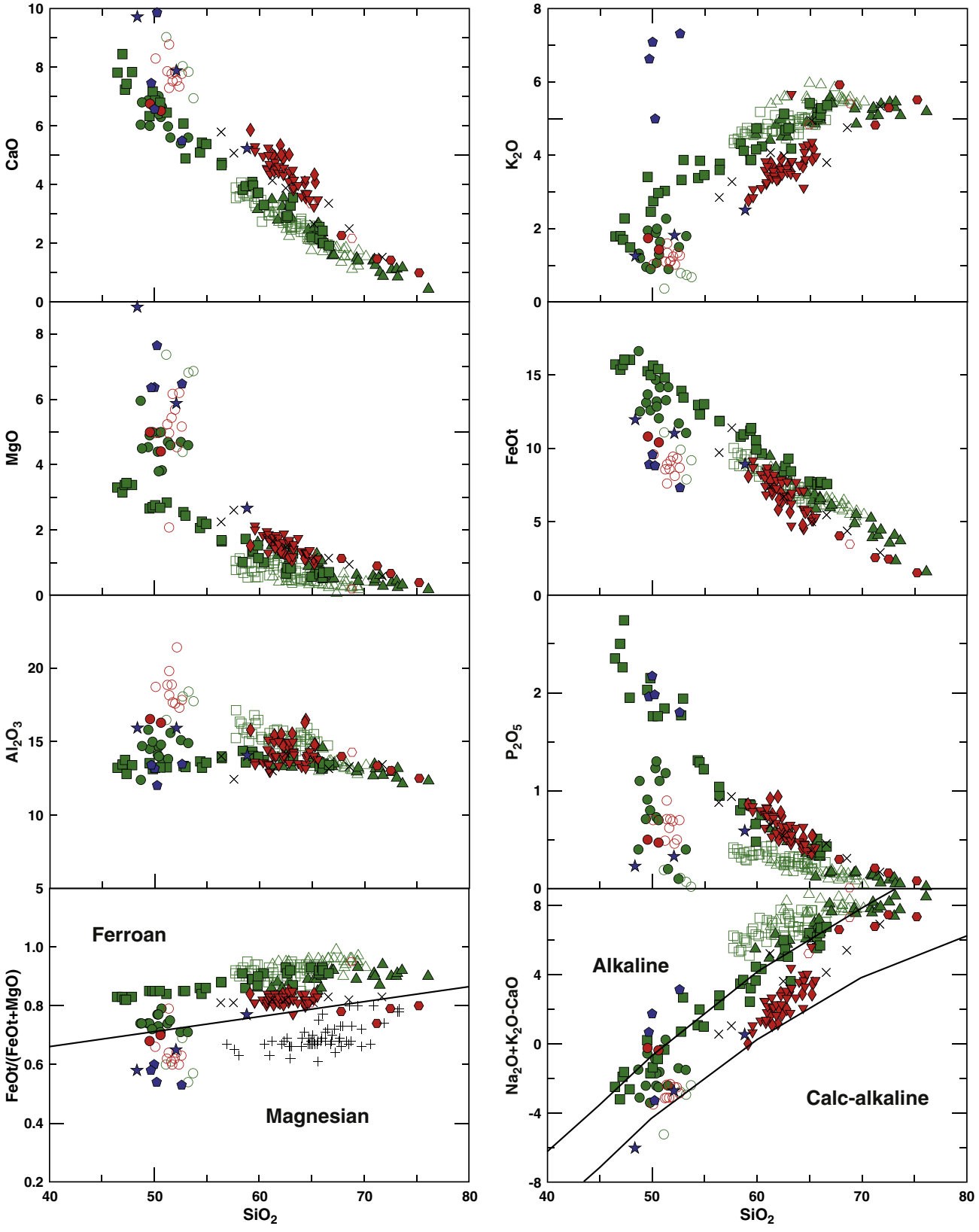
CaO
MgO
Al2O3
FeOt/(FeOt+MgO)
Ferroan
Magnesian
SiO2
K2O
FeOt
P2O5
Na2O+K2O-CaO
Alkaline
Calc-alkaline
SiO2
HBG suite
Gabbronorites
Mafic enclaves
Lyngdal
Valle
Tranevag
Svöfjell
Red granite
AMC suite
High-Al gabbros
Primitive jotunites
LLD
OLT
APT
PXT
Feda suite
Amphibolitic enclaves
UltraK enclaves
Augen gneiss

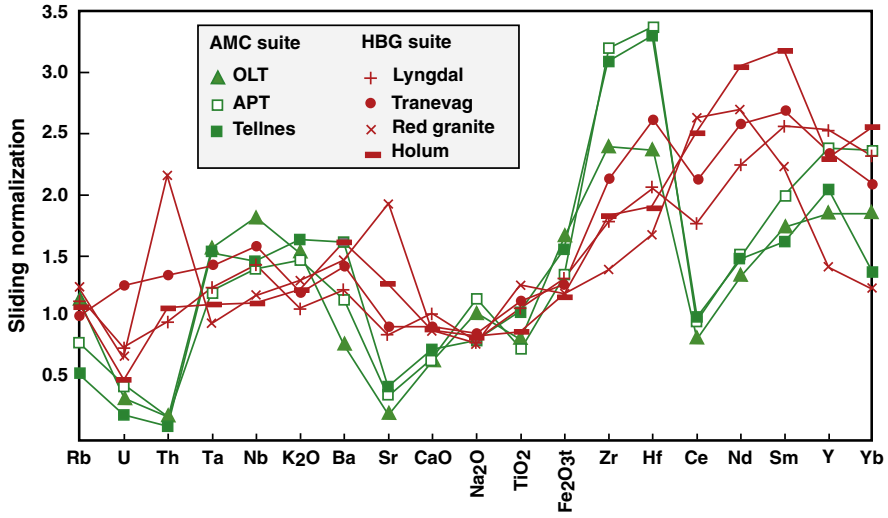

Fig. 6. Spider diagrams normalized to the Yenchichi 2–Telabit series (sliding normalization) of Liégeois et al. (1998). In this normalization, the trace element content of one sample is divided by the trace element content in the reference series (Yenchichi 2–Telabit series) at the same SiO_2 content. The data shown for each intrusion correspond to the average of normalized values of all available samples.

contaminant was initially defined by Andersen et al. (1994). It corresponds to the source region of the Ubergsmoen metacharnockite (1.12 Ga), an augen gneiss unit emplaced in the Bamble sector and belonging to the Gjerstad suite (1.19–1.13 Ga) (Bingen and van Breemen, 1998a). The Sr and Nd isotopic trends of the group 1 granites has been predicted by mixing of a primitive component and this crustal contaminant C2 (Andersen et al., 2001).

The intermediate and acidic members of the Feda augen gneisses mimic the trend of the HBG suite in the ε_{Nd}-Sr_i and $^{206}Pb/^{204}Pb$–$^{207}Pb/^{204}Pb$ (Fig. 7) diagrams indicating that contamination in this magmatic suite has involved the same contaminant C2. Interestingly, the mafic facies of the Feda suite have initial Sr, Nd and Pb isotopic compositions which are very similar to those of the mafic facies of the HBG and AMC suites (Fig. 7). In the $(^{206}Pb/^{204}Pb)_i$–$(^{207}Pb/^{204}Pb)_i$ diagram (Fig. 7), the ultrapotassic enclave (sample 117b of Bingen et al., 1993: Table 3) has initial Pb isotopic compositions, calculated at 1.05 and 0.93 Ga, which overlap with the isotopic compositions of the HBG and AMC mafic facies, whereas the amphibole-rich enclaves have lower Pb isotopic ratios indicating the involvement of the C2 contaminant. In the Sr_i–ε_{Nd} diagram (Fig. 7), the reverse same situation is observed. One of the amphibole-rich enclaves (sample BB82b: Table 2) has Sr and Nd isotopic compositions which overlap those of the HBG and AMC mafic facies whereas the ultrapotassic enclaves have lower ε_{Nd} suggesting the involvement of the C2 contaminant.

5. Discussion and geological implications

5.1. Structure of the Sveconorwegian continental crust

The differentiation trends outlined by the three suites (AMC, HBG, Feda) in the ε_{Ndt}–Sr_i and $(^{206}Pb/^{204}Pb)_i$–$(^{207}Pb/^{204}Pb)_i$ diagrams indicate two contrasting older crustal contaminants, as already stressed by Andersen et al. (2001), Bolle et al. (2003a) and Vander Auwera et al. (2008). The C2 crustal contaminant of the HBG and Feda suites is characterized by low Rb/Sr, U/Pb and Sm/Nd ratios. An old granulitic crust, depleted in U and Rb during its granulitic dehydration, is a plausible candidate. The mean Nd T_{DM} of the HBG suite is around 1.6 Ga (see Andersen et al., 2001; Vander Auwera et al., 2003), an intermediate age between the primary component, the component observed in the least differentiated facies of the three suites, and the old contaminant, which suggests that this later component should be older than 1.6 Ga. In the AMC suite, the crustal contaminant C1 is characterized by higher Rb/Sr, U/Pb and Sm/Nd ratios than the C2 contaminant. Based on the Nd T_{DM} model ages of the AMC suite (mean: 1.6 Ga: see Bolle et al., 2003a), this C1 contaminant should also have an age older than 1.6 Ga. Moreover given its high Sr isotopic ratio at 0.93 Ga, its Rb/Sr ratio was not decreased during an old granulitic dehydration process as it was for contaminant C2. The hypothesis that crustal contaminants C1 and C2 could be older than 1.6 Ga is in agreement with results from Andersen et al. (2001) and Andersen et al. (2002b). Indeed, based on the Sr–Nd–Pb–Hf isotopic compositions of their group 1 granites, these authors concluded that these granites display evidence of a crustal component having a crustal history extending back to 1.7–1.9 Ga. However, no rocks older than 1.55 Ga have been found in the Telemarkia terrane (Bingen et al., 2005).

The identification of two different crustal contaminants with different metamorphic histories in the HBG and AMC suites has implications for the structure of the Sveconorwegian continental crust. Indeed, this suggests that these two contaminants could correspond to two major lithotectonic units in which the AMC and HBG suites were emplaced. A Moho offset recognized southeast of the Rogaland anorthositic complex (Andersson et al., 1996) could be interpreted as the trace of a major crustal boundary (Duchesne et al., 1999). Duchesne et al. (1999) proposed that this boundary may be marked by the Feda augen gneiss in the same way as augen gneiss marks the southern part of the Mandal–Ustaoset Line (Sigmond, 1985) (Fig. 1). Bolle et al. (2010) discuss in detail the exact location of a crustal lineament possibly linked to the Moho offset. The observation that the south Rogaland Anorthosite Province appears to be devoid of rocks belonging to the HBG suite that contain the C2

Fig. 5. Major elements composition of the Feda (Bingen et al., 1993), AMC (OLT, PXT for the upper part of Bjerkreim–Sokndal intrusion (Duchesne and Wilmart, 1997); APT for the Apophysis (Bolle and Duchesne, 2007); AMC mafic facies (Duchesne et al., 1987b; Robins et al., 1997; Vander Auwera et al., 1998; Bolle et al., 2003a); LLD (Wilmart et al., 1989; Vander Auwera et al., 1998)) and HBG (Svöfjell, gabbronorites, Lyngdal, Tranevag, Red Granite, Mafic enclaves, Valle: Demaiffe et al., 1990; Bogaerts et al., 2003a; Vander Auwera et al., 2003) suites. Reference lines in $FeO_t/(FeO_t + MgO)$ and $Na_2O + K_2O$–CaO are from Frost et al. (2001) and Frost and Frost (2008). Data for the Feda augen gneisses are shown only in the FeO_t–SiO_2 plot. See Bingen (1989) and Bingen et al. (1993) for a detailed account of the augen gneisses geochemistry.

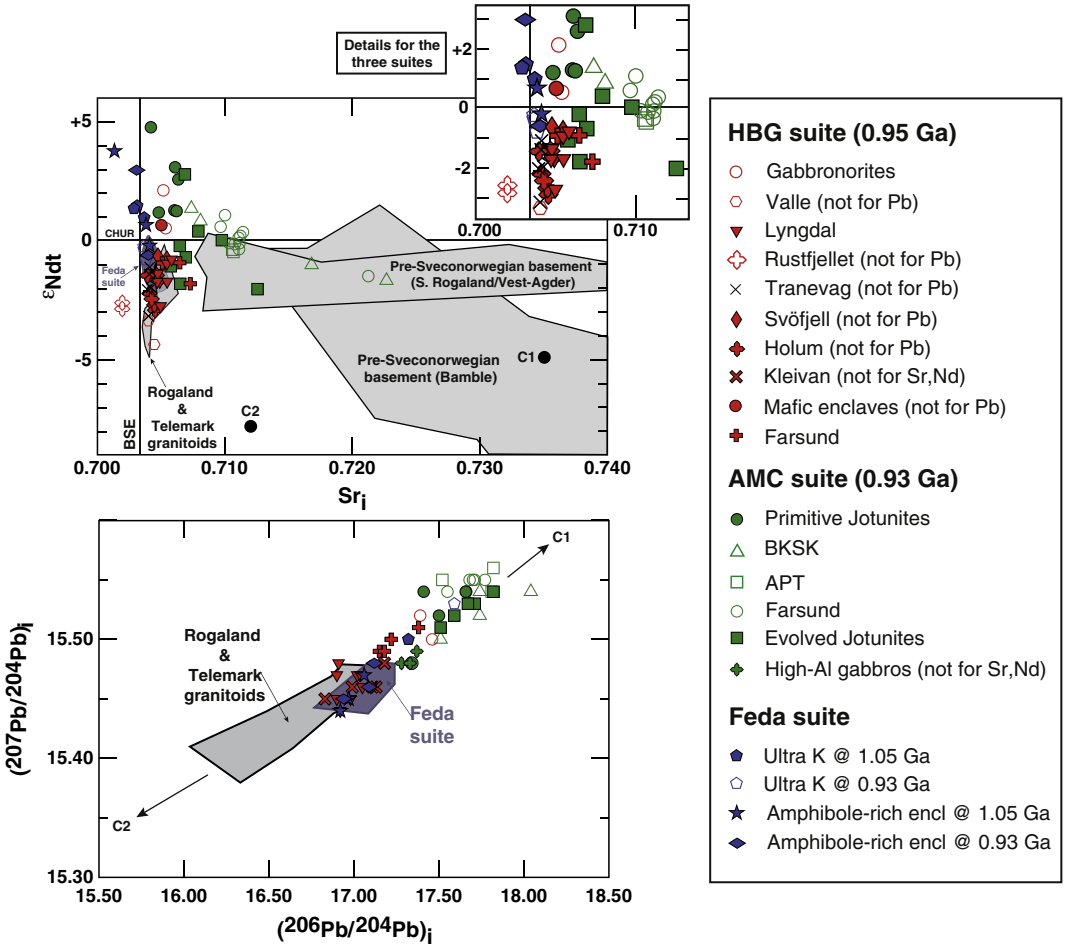

Fig. 7. Initial Pb, Sr and Nd isotopic compositions for the HBG, AMC and Feda suites. Isotopic compositions have been recalculated back to the emplacement age of the different suites: 0.93 Ga for AMC, 0.95 Ga for HBG and 1.05 Ga for Feda. Pb isotopic data from Weis (1986), Demaiffe et al. (1990), Bingen et al. (1993), Barling et al. (2000), Andersen et al. (2001), Dupont (2003) and Dupont et al. (2005). Sr and Nd isotopic data from Demaiffe et al. (1990), Bingen et al. (1993), Andersen et al. (2001), Bogaerts et al. (2003a), Vander Auwera et al. (2003) and Dupont et al. (2005). Evolution of bulk silicate Earth (BSE) is calculated back from present ratios of $^{87}Sr/^{86}Sr = 0.7047$ and $^{87}Rb/^{86}Sr = 0.0850$ (Faure, 1986).

signature, whereas the region bearing the HBG granitoids lack AMC rocks with the C1 signature supports this hypothesis.

5.2. Lower crustal sources of the HBG and AMC mafic facies

The comparable composition of the mafic facies of the AMC (primitive jotunites, high-Al gabbros) and HBG (gabbronorites) suites was previously noted by Demaiffe et al. (1990), Vander Auwera et al. (2003) and Vander Auwera et al. (2008). As shown above, this similarity is also true for Sr, Nd and Pb isotope data. All three isotopic systems point to a source, here referred to as the primary component, having only a minor participation of old continental crust. This is particularly evident from the Pb isotopic signatures, which are very sensitive to contamination by old crust. Given the largely overlapping Sr, Nd and Pb isotopic compositions of the mafic facies in both suites, we consider that this primary component is the same in the two suites. Using experimental data acquired on plausible parent magmas of massif-type anorthosites including primitive jotunites and high-Al gabbros, Longhi et al. (1999) and Longhi (2005) showed that these compositions lie on thermal highs in relevant phase diagrams and that consequently these parent magmas were produced by melting of lower crustal sources rather than by fractionation of mantle melts (see Section 4.1.3). This hypothesis was extended to the gabbronorites, parent magmas of the HBG suite, because their compositions are close to those of primitive jotunites (Vander Auwera et al., 2008). The isotopic and experimental constraints thus support the hypothesis that the mafic facies of the two suites were produced by partial melting of lower crustal sources that had the same isotopic composition. We will now evaluate the mafic magmatism events which could possibly generate the primary component of these post-collisional magmatic suites. For this we will consider the events belonging to the SW part of the Fennoscandia shield and that are older than the HBG and AMC suites.

The main events of Mesoproterozoic mafic magmatism in South Norway (Fig. 1) include the 1.05 Ga Feda suite mafic facies as well as the volcanic sequences of Gjuve–Morgedal (1.16 Ga, central Telemark), Valldal (1.26 Ga, Rogaland–Hardangervidda) and Vemork (1.50 Ga, central Telemark). As summarized in Section 4.1.1., the Feda suite displays a typical high-K calc-alkaline orogenic trend which possibly represent subduction related granitoids or syn-collisional granitoids emplaced during the late Sveconorwegian orogenic phase (Bingen et al., 2005). The Gjuve–Morgedal metabasalts belong to the Høydalsmo group of the Telemark supracrustal sequence (Dons, 1960; Laajoki et al., 2002). Similarly, the Valldal metabasalts are part of the Valldal volcano-sedimentary sequence that is considered as a possible equivalent of part of the Telemark supracrustal belt in the Rogaland–Hardangevirdda. Brewer et al. (2002) and Brewer et al. (2004) related the Gjuve–Morgedal and Valldal metavolcanics to a long-lived convergent margin based on their Nd isotopic composition and the presence of a negative Nb anomaly in their primitive mantle normalized spider diagrams. Brewer et al. (2002) and Brewer et al. (2004) inferred that they were emplaced in an environment of

continental back-arc extension related to subduction along the western margin of Baltica. Bingen et al. (2003) discussed the possibility that the Gjuve–Morgedal metabasalts belonged to an environment similar to the one of the Basin and Range Province. They proposed that this mafic volcanism took place in the context of an extensional to transtensional regime that possibly followed cessation of a subduction regime. The older Vemork metabasalts are part of the Rjukan group of the Telemark supracrustal belt. These metabasalts extruded during an important magmatic event dated at 1.52 to 1.48 Ga that represents a major continental growth whose geotectonic setting is not clear (Bingen et al., 2005). The Sr isotopic composition of the Vemork, Valldal and Gjuve–Morgedal metabasalts has been disturbed during the Sveconorwegian greenschist facies metamorphism (Brewer et al., 2002, 2004), so only Nd isotopes will be used to evaluate if these formations could potentially represent the source of the primary component of the HBG and AMC suites. A summary of Nd isotopic compositions is shown in Fig. 8. ε_{Nd} and the evolution of these potential sources are compared with the HBG and AMC mafic facies at 0.95 and 0.93 Ga, respectively. In the case of the oldest event, the Vemork formation, the ε_{Nd} of most mafic facies is too low to account for the Nd isotopic compositions of the HBG and AMC suites. Also, model ages obtained for the AMC suite do not support the oldest event. Indeed, as discussed by Bolle et al. (2003a), the least differentiated compositions of the AMC suite (primitive jotunites and anorthosites) have young model ages (Nd T_{DM}) ranging from 1.35 to 1.10 Ga, which imply a short crustal residence time (less than 0.2–0.4 Ga: Bolle et al., 2003a). Similarly, in the HBG suite, the Tovdal granitoid (0.94 Ga, $Sr_i = 0.70427$, $\varepsilon_{Ndt} = +4.4$) has a young T_{DM} model age of 1.03 Ga (Andersen et al., 2001, 2002a. The ε_{Nd} of the mafic facies of the Valldal and Gjuve–Morgedal formations are high enough to account for the Nd isotopic composition of the HBG and AMC suites contrary to the mafic facies of the Feda suite that display too low ε_{Nd}. Nevertheless, two observations favor the Feda mafic facies as sources for the AMC and HBG suites: 1) the Sr and Pb isotopic compositions are very similar to those of the mafic facies of the HBG and AMC suites; 2) the Feda suite is the youngest event preceding the emplacement of the AMC and HBG suites. Consequently, in the current state of knowledge, the Feda suite mafic facies, as well as the Valldal and Gjuve–Morgedal metabasalts are considered as candidates. It is worth noting that even if the geodynamic context of these events remains of course speculative, it seems that they are related in space and time to a subduction event. This is in agreement with what is currently known about the anorthosites of the Grenville Province. There, most workers favor an active margin environment (e.g. Rivers and Corrigan, 2000). Moreover, Bédard (2010) recently inferred that a range of parental melts is needed to account for the petrogenesis of the Grenvillian anorthosites and that at least part of these melts result from extensive high pressure partial melting of arc basaltic sources.

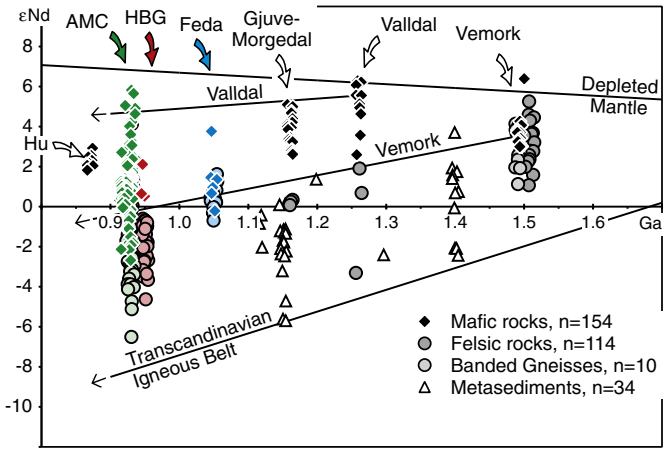

Fig. 8. Nd versus time for the main characterized Mesoproterozoic mafic magmatism in the Telemarkia Terrane: 1.50 Ga Vemork volcanism (central Telemark: Brewer and Menuge, 1998), 1.26 Ga Valldal volcanism (1.26 Ga Rogaland–Hardangervidda: Bingen et al., 2002; Brewer et al., 2004), 1.16 Ga Gjuve–Morgedal volcanism (central Telemark: Zhou et al., 1995; Brewer et al., 2002; Laajoki et al., 2002), 1.05 Ga Feda mafic enclaves facies (Rogaland–Vest Agder) (Bingen et al., 1993; Bingen and van Breemen, 1998a), metasediments (deHaas et al., 1999; Andersen and Laajoki, 2003), banded gneiss (Menuge, 1988; Vander Auwera et al., 2003), Hunnedalen dyke swarm (Hu) (Menuge, 1988; Vander Auwera et al., 2003), HBG and AMC (see Fig. 7). The evolution of Nd versus time has been calculated with the average $^{147}Sm/^{144}Nd$ of the different magmatisms: 0.145 for Vemork, 0.177 for Valldal and 0.107 for the granitoids of the Transcandinavian Igneous Belt. The depleted mantle has been calculated with the model of DePaolo et al. (1991).

5.3. Relation between the Sveconorwegian metamorphism and the composition of the lower crustal sources

As already mentioned, the mafic facies of the AMC and HBG suites have similar geochemical and isotopic signatures. The differences observed between the two suites with increasing SiO_2 (Figs. 5 and 6), namely higher CaO and Sr as well as lower K_2O and FeO_t/MgO in the HBG suite, can be attributed to the subtraction of different cumulates during differentiation (e.g. Wilmart et al., 1989; Vander Auwera et al., 1998; Vander Auwera et al., 2008). However, the AMC suite is anhydrous (orthopyroxene) whereas the HBG suite is hydrous (amphibole and biotite: Bogaerts et al., 2006; Vander Auwera et al., 2008). We also emphasized that although fO_2 probably covers overlapping ranges of values in both suites (FMQ-1 to NNO in AMC and NNO to NNO + 1 in HBG, see Section 4.1.3), fO_2 was lower in the AMC suite. We will now discuss the possibility that these differences in H_2O content and fO_2 may have been induced by the varying grade of the Sveconorwegian metamorphism on the sources (HBG and AMC) (Vander Auwera et al., 2008).

The Sveconorwegian metamorphism started at 1.035 Ga, shortly after the emplacement of the youngest mafic magmatism event, the Feda suite (1.05 Ga). The grade of this regional metamorphism increases from greenschist facies in Telemark in the northeast to granulite facies in Rogaland–Vest Agder in the southwest. There, these high grade conditions were maintained until 0.973 Ga as indicated by molybdenite Re–Os dating (Bingen and Stein, 2003). The isograd pattern of the Sveconorwegian regional metamorphism thus indicates that the highest thermal anomaly was centered on the Rogaland–Vest Agder. Moreover, as mentioned above (see Section 2), geochronological data demonstrate that a granulite basement was present in Rogaland at the end of the regional metamorphism (0.97 Ga). Additionally, the opx-bearing assemblages that were dated at 0.97 Ga, were formed in the upper crust at 0.55 GPa (Bingen and Stein, 2003). This suggests that the opx-in isograd may not have been originally parallel to the MOHO. This hypothesis is supported by heat flow modeling that shows that modern isotherms are dome-shaped along a section extending from southern Norway to northern Denmark (Balling, 1985). Consequently, we suppose that in the Sveconorwegian lower crust, amphibolite facies conditions prevailed east of the opx-in isograd and granulite facies conditions, west of this isograd.

We suggest that the granulitic lower crust west of the opx-in isograd produced an anhydrous source for the AMC suite while leaving a slightly hydrated source (Vander Auwera et al., 2008) for the HBG suite east of the opx-in isograd. An anhydrous source is necessary to produce the AMC suite. Indeed, if the source of the parent magma of the AMC suite contained H_2O, this water would have been concentrated in the melt during dehydration partial melting, thus producing an H_2O-bearing parent magma which is inconsistent with the anhydrous character of the whole AMC suite. The interaction between H_2O and oxygen fugacity is difficult to assess without direct evidence of the metamorphic reactions that took place in the lower

crust. As pointed out by Vander Auwera et al. (2008), Beard and Lofgren (1991), who estimated the oxygen fugacity at NNO + 1 and NNO + 2 using coexisting magnetite and ilmenite, noted that dehydration melting of amphibolite produced lower fO_2 in their charges than water-saturation melting. Hence, it is possible that more extensive dehydration produced a more reduced lower crustal source for the AMC suite. Granulitization may also be responsible for the lower U, Th and Rb contents of the AMC mafic facies compared to the mafic facies of the HBG suite (TJ primitive jotunite: U = 0.2 ppm, Th = 0.5 ppm, Rb = 18 ppm, Vander Auwera et al. (1998): HBG mafic enclaves: U = 0.6–0.5 ppm, Th = 1.69–2.9 ppm, Rb = 57–45 ppm, Bogaerts et al. (2003a)) (Rudnick et al., 1985).

In summary, we suggest that abundant mafic magmas were emplaced at the base of the crust during a previous event (1.26–1.05 Ga) possibly related to activity along a long-lasting convergent margin. Later, this underplated lower crust was affected by the Sveconorwegian regional metamorphism (1.035–0.97 Ga) with production of a dehydrated reduced lower crust west of the opx-in isograd and a still hydrated more oxidized mafic lower crust east of the opx-in isograd. Shortly after the end of the regional metamorphism, at 0.97 Ga, the post-collisional magmatism was produced by partial melting of these lower crustal sources and yielded the parent magmas of the HBG and AMC suites (Fig. 9).

5.4. Exhumation or unroofing rates of the Sveconorwegian orogeny

Exhumation rates can be estimated in two independent ways, one using the magmatic suites and the other using metamorphic equilibria combined with geochronology. At 1.006 Ga, the metamorphic gneisses near Lyngdal recorded an estimated pressure of 0.6–0.8 GPa (Möller et al., 2002). At 0.95 Ga, the Lyngdal intrusion was emplaced in these gneisses at 0.2–0.4 GPa (Bogaerts et al., 2006). Thus an equivalent of about 0.4 GPa of crust was lost in 56 Ma which yields an estimated exhumation rate of 12 km/56 Ma or 0.21 mm/y. When the uncertainty on the pressure is taken into account, the exhumation rate ranges from 0.10 to 0.32 mm/y.

The pressure conditions of the M1 phase of the Sveconorwegian metamorphism have been constrained at 0.6–0.8 GPa at 1.035 Ga. The time of decompression to 0.56 GPa was further estimated at 0.955 Ga by Tomkins et al. (2005) using zircon grains that co-crystallized with cordierite rims surrounding garnet. Given the pressure range of M1, this gives an exhumation rate of about 0.02 to 0.1 mm/y.

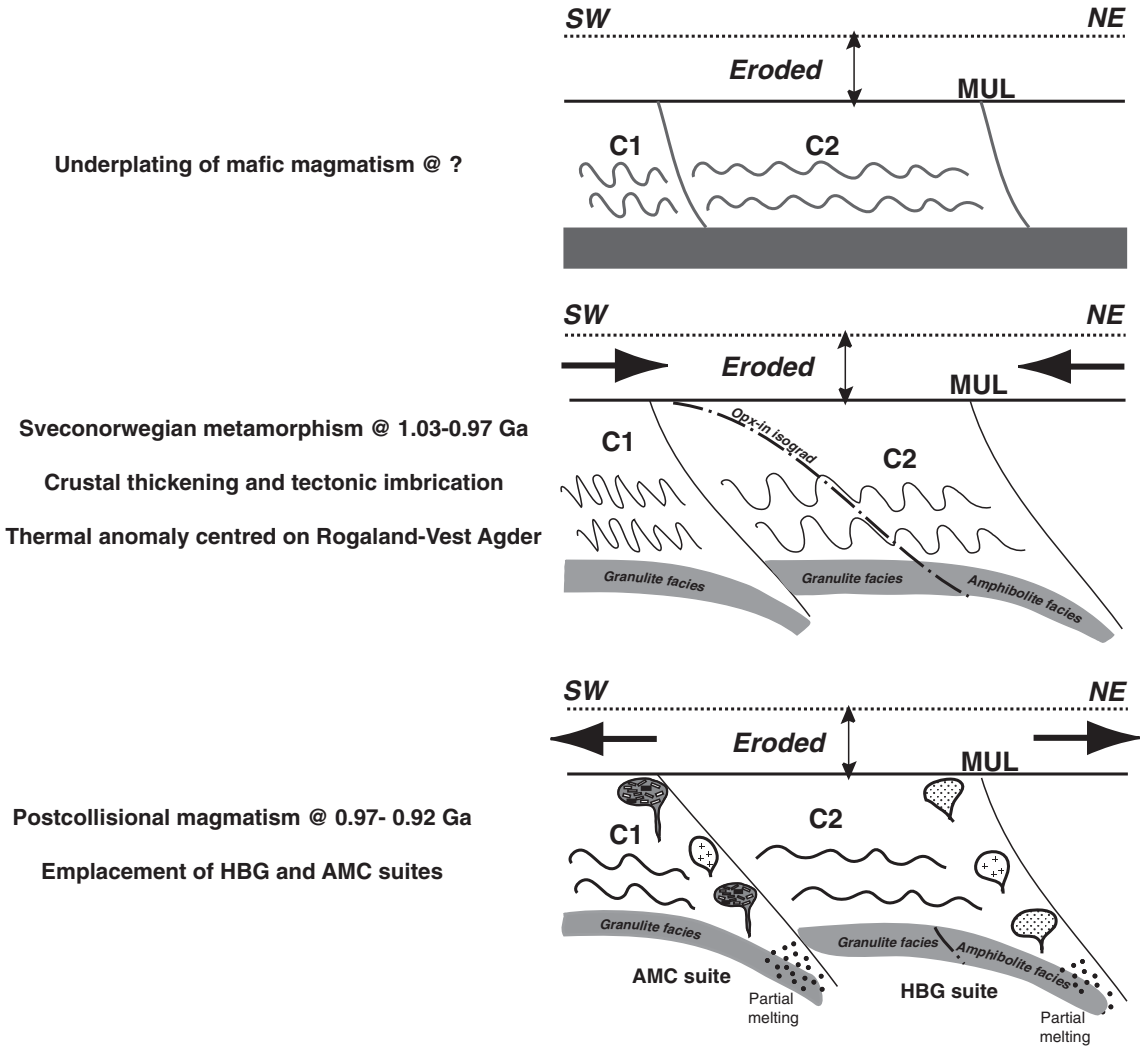

Fig. 9. Conceptual sketch across the Sveconorwegian orogen from the Rogaland AMC suite to the Mandal–Ustaoset line (MUL). C1 and C2 represent the two lithotectonic units recognized in the isotopic composition of the HBG and AMC suites. They are separated by a crustal boundary (Bolle et al., 2010) (see text for explanation). Different symbols are used for anorthositic diapirs (dark gray) and acidic intrusions (crosses) in the AMC suite and for intermediate (dots) and leucogranitic (crosses) magmas in the HBG suite. In this conceptual sketch, partial melting of the lower crust is made possible by underthrusting of lower crustal tongues into the mantle. However, other processes such as foundering of overdense lower crustal sources in the upper mantle are also possible (see text for explanation).

These estimated exhumation rates are low (1 mm/y being considered as rapid) and provided time for the crust to be heated.

There is evidence that the Sveconorwegian orogen was exhumed by both erosion and thinning (extension). Foreland basins that could store products of erosion are conspicuously lacking in front of the Sveconorwegian orogen on Fennoscandia (see Bingen et al., 2008). Nevertheless, large and thick sedimentary basins, formed after 1.03 Ga at the northern margin of Baltica and Laurentia — now exposed in the Caledonides of Svalbard, East Greenland, Finnmark, Scotland and Shetland — are interpreted as distal basins collecting sediments sourced in the combined Grenvillian and Sveconorwegian mountain belts (Cawood et al., 2010). Modeling by England and Thompson (1986) showed that crustal thinning of large collision areas may occur by extensional strain as the orogen collapses under its own weight. Extensional reactivation of major shear zones is documented in the Sveconorwegian orogen (Mulch et al., 2005). Also, distribution of titanite U–Pb and molybdenite Re–Os ages led Bingen et al. (2006) to suggest that the amphibolite- to granulite-facies domain of the Rogaland Vest Agder could correspond to a gneiss dome (Corti et al., 2003) progressively exhumed during the extension regime prevailing in the post-collisional evolution of the Sveconorwegian orogeny after 0.97 Ga.

5.5. Timing of the Sveconorwegian post-collisional magmatism

The new U–Pb zircon geochronological data acquired on a selection of samples bring additional constraints on the timing of intrusion of the two post-collisional magmatic suites. In the Telemarkia terrane, post-collisional plutons forming the HBG suite range in age between 970 and 932 Ma. The new data corroborate the data by Schärer et al. (1996) indicating just two magmatic pulses in the whole AMC suite. The main magmatic pulse took place at 933–929 Ma, leading to formation of the massif-type anorthosites, satellite leuconorite plutons (Hidra pluton), the Bjerkreim–Sokndal layered intrusion and a number of minor occurrences of monzonorite (Eia–Rekefjord intrusion, Tellnes dyke). A second minor magmatic pulse at 920–916 Ma corresponds to intrusion of jotunitic magmas and related acidic melts in dykes (Tellnes ilmenite norite, Lomland dyke) and at the roof of the Bjerkreim–Sokndal intrusion resulting in crystallization of part of the mangerite–charnockite sequence of this intrusion. These new geochronological data thus also confirm the composite nature of the Bjerkreim–Sokndal intrusion.

The geochronological data also indicate that emplacement of the HBG suite started before the formation of the AMC suite, lasted about twice as long (38 Ma compared to 17 Ma) as the AMC suite and ended when the main pulse of the AMC suite took place. Also, the HBG suite covers nearly all of southern Norway, a much larger surface than the exposed AMC suite. Although, part of the Rogaland intrusive complex may lie offshore in the Skagerrak Sea under a thick cover of sediments (Olesen et al., 2004). We attribute the earlier formation of the HBG suite to the lower temperature necessary to melt a slightly hydrated source compared to a completely anhydrous source. This difference in melting temperature is probably also responsible for the shorter time span of the AMC suite as the very high temperature required to melt the anhydrous gabbronoritic source could only be reached during peak conditions.

5.6. Why were massif-type anorthosites produced in the AMC suite and not in the HBG suite?

Given that the mafic facies of both suites have similar compositions, it is puzzling to observe that massif-type anorthosites have been produced only in the AMC suite.

Geochemical modeling and experimental data indicate that differentiation from the primitive jotunites, parent magmas of the Rogaland andesine anorthosites, to the evolved jotunites can be accounted for by fractional crystallization with subtraction of a leuconoritic cumulate. This early differentiation process is constrained to have occurred in lower crustal magma chambers by the presence of high Al orthopyroxene megacrysts that characterize the massif-type anorthosites. The calculated (Duchesne, 1978) and experimental (Vander Auwera and Longhi, 1994; Vander Auwera et al., 1998) leuconoritic cumulate contains a very high proportion of plagioclase (74%) greatly favoring the buoyant segregation of a crystal mush (e.g., Longhi et al., 1993). This high proportion of plagioclase was enhanced by the anhydrous character of the magma that expanded the stability field of plagioclase. Indeed, H_2O, when present, depolymerizes the silicate melt and thus lowers the liquidus temperature of silicates. Moreover, the anorthosites were emplaced west of the opx-in isograd in the warmest and most ductile part of the orogen. High temperatures would have facilitated the ascent of the magmatic diapirs through a plastically deforming continental crust.

Using geochemical modeling, Vander Auwera et al. (2008) showed that the monzodioritic liquids of the HBG suite could be produced either by fractional crystallization of a liquid with the composition of an HBG mafic facies or by partial melting of a mafic source. When partial melting was tested, it was supposed that the mafic source had a composition equivalent to that of the mafic facies recognized in the HBG suite. In other words, younger sills emplaced in the lower crust remelt slightly older sills. In the following, the possibility of producing anorthositic diapirs will be examined for both processes. 30% partial melting of a mafic source in the lower crust can generate a monzodioritic liquid and 70% mafic restite. These monzodioritic liquids are probably too evolved (Mg# = 0.29: Bogaerts et al., 2003a) to be plausible anorthosite parent magmas. Additionally, mass balance calculations using the least-squares method indicate that differentiation of these monzodioritic liquids to produce granodioritic liquids can be accounted for by subtraction of a bulk cumulate containing a low proportion of plagioclase: 47% or 56% (Bogaerts et al., 2003a). In the case of fractional crystallization, it is possible to reach monzodioritic liquids by subtracting a cumulate made of 53% plagioclase from the mafic parent magma. This cumulate composition was obtained from the experimental data of Sisson et al. (2005) acquired on mildly hydrated mafic compositions. A small amount of H_2O in the mafic facies of the HBG suite was necessary to reach amphibole saturation in the intermediate monzodioritic composition. This small amount of water probably reduces the stability field of plagioclase and increases that of amphibole, thus producing an early cumulate with a much lower proportion of plagioclase than in the anhydrous mafic facies of the AMC suite. This much lower proportion of plagioclase probably precluded the development of a sufficiently buoyant instability to form magmatic diapirs. Moreover, the HBG suite is located on the low-temperature side (east) of the opx-in isograd. The temperature in the lower crust was thus lower than in the case of the AMC suite, also hindering plastic deformation necessary for diapiric ascent.

5.7. Why are massif-type anorthosites restricted to the Proterozoic?

Using available petrological models on the AMC and HBG Sveconorwegian post-collisional suites, we suggest that the parent magmas of these two suites were produced by partial melting of a source emplaced in the lower crust during a previous mafic magmatic event that has yet to be clearly identified. We can thus address the conditions which, according to this model, were necessary for the development of massif-type anorthosites in the AMC suite:

1. Abundant underplated mafic magmatism;
2. Regional metamorphism reaching granulite facies conditions is a prerequisite as it produces the necessary anhydrous lower crustal source for the AMC suite;

3. Melting of the lower crustal sources: first in the HBG suite (0.97–0.93 Ga) as the melting temperature is lower (hydrous lower crust) and second in the AMC suite (0.93 Ga);
4. The mafic facies so produced are the starting points of the two magmatic suites with production of massif-type anorthosites in the AMC suite.

It has long been recognized that massif-type anorthosites are characteristic of the Proterozoic and geochronological data have shown that they range from 2.12 Ga (Arnanunat, Canada: Hamilton et al., 1998; Ryan et al., 1999) to 0.93 Ga (Rogaland, Norway: Schärer et al., 1996). The model proposed here may help to understand this observation. The Earth is a cooling body and even if arguments that in the Archean the mantle was not as warm as initially supposed are true (Parman et al., 1997, 2003), estimates still indicate temperatures 100 °C higher than in the Phanerozoic (Grove and Parman, 2004). In the Proterozoic, the Earth's mantle was thus probably also warmer than in the Phanerozoic and this has already been proposed by several authors as an explanation of the Proterozoic age of the massif-type anorthosites (e.g. Ashwal, 1993; Bédard, 2010). In our model, we consider that very high temperatures are needed to remelt the lower crust. The question remains as to why anorthosites were not formed in the Archean when the mantle was even warmer? It is possible that the answer to this question lies with the first prerequisite mentioned above, the previous underplating of subduction-related mafic magmas. Indeed, this prerequisite implies that subduction was operating similarly as today with production of basalts in the metasomatized mantle wedge or in continental back-arc setting followed by their underplating beneath a thick continental crust. In the Archean, when the mantle was warmer, experimental and geochemical data indicate that the subducted basaltic slab probably melted instead of dehydrated (e.g. Martin, 1986; Rollinson, 2007). Accordingly, felsic magmas (tonalites, granodiorites) were transferred from the subducted slab to the crust impeding the production of abundant underplated basalts. It is also possible that because of secular cooling, during the Archean, the Earth was able to produce large mafic to ultramafic layered intrusions, like the Stillwater complex (2.7 Ga) (many of these mafic plutonic bodies were probably trapped in the lower crust because of their high density) and subsequently in the Proterozoic, less heat was available thus lessening the formation of these ultramafic intrusions, but still enough heat was available to remelt them and produce the parent magma of the massif type anorthosites by their foundering in the upper mantle (Longhi et al., 1999; Longhi, 2005). The amount of continental crust present at the start of anorthositic magmatism may also have played a role as a thick continental crust is demanded by the pressure of crystallization of the high-Al orthopyroxene megacrysts (1.1–1.3 GPa). Bédard (2010) also suggested that the pre-Proterozoic crust was not strong enough to be tectonically thickened. As summarized by Rollinson (2007), several lines of evidence suggest indeed that before 2 Ga the volume of continental crust was relatively small. The mantle evolution curve of ε_{Nd} versus time (Nagler and Kramers, 1998) started to increase from about +1 at the end of the Archean. This increase can be linked to the extraction of the continental crust supporting the inference that the amount of continental crust was limited before the Late Archean. Also, the beginning of the secular variation of the mantle U/Pb at about 2 Ga has been explained by the built-up of a significant volume of continental crust (Elliott et al., 1999). Finally, several isotopic systems suggest that after 3 Ga the nature of mantle processes probably changed (Rollinson, 2007). Consequently, the onset of massif-type anorthosites magmatism may indicate when plate tectonics began to operate in a way similar to today.

6. Conclusions

New and published U–Pb zircon geochronological data bracket the emplacement of the HBG suite between 970 and 932 Ma and confirm a short lived intrusion of the AMC suite, with a major pulse at 933–929 Ma and a minor pulse at 920–916 Ma.

Published Sr–Nd–Pb isotopic data on the Feda, HBG and AMC suites as well as new data on three mafic facies of the Feda orogenic suite indicate the involvement of three end-members in these magmatic suites: the parental mafic facies (primary component) and two different crustal contaminants. The C2 crustal contaminant involved in the HBG (Andersen et al., 2001) and Feda suites is characterized by low Rb/Sr, U/Pb ratios and Sm/Nd, and was probably a granulitic crust depleted in U and Rb. The C1 crustal contaminant involved in the AMC suite and already recognized by Bolle et al. (2003a) is characterized by higher Rb/Sr, U/Pb and Sm/Nd ratios. It is proposed that these two crustal contaminants correspond to two different lithotectonic units possibly separated by a recently recognized shear zone located just East of the AMC suite (Bolle et al., 2010).

Given that the primary component is the same in the HBG and AMC suites, we suggest that the parent magmas of both suites were produced by partial melting of lower crustal sources formed at the base of the crust during a previous mafic magmatic event. Possible candidates for this latter are the Valldal and Gjuve–Morgedal metabasalts (1.26 and 1.16 Ga), interpreted as related to a long lived convergent margin and the mafic facies of the Feda orogenic suite.

Prior to partial melting, the granulite facies Sveconorwegian regional metamorphism played a key role in modifying the composition of the lower crustal sources west of the opx-in isograd where the AMC suite was emplaced. Specifically, the granulite facies conditions produced the appropriate anhydrous source for the parent magmas of the AMC suite. In turn, the anhydrous character of these magmas expanded the stability field of plagioclase enabling the early crystallization of a high proportion of this phase and formation of gravitationally unstable anorthositic diapirs.

According to this model, the anorthosites are formed during the post-collisional evolution of the orogen by partial melting of the continental arc root. This process was made possible in the Proterozoic because the temperature was sufficiently high to promote partial melting of an anhydrous mafic lower crust. Such a process did not occur in the Archean because the main mass transfer to the crust was then felsic (tonalites, granodiorites — melting of the subducted slab) and not basaltic (dehydration of the subducted slab), thus precluding the formation of the prerequisite lower crustal sources in the continental arc root. Therefore onset of massif-type anorthosites magmatism may indicate a plate tectonic regime similar as today.

Acknowledgments

The NORDSIM facility in Stockholm is operated under an agreement between the research funding agencies of Denmark, Norway, Sweden and Finland, the Geological Survey and the Swedish Museum of Natural History. Data were collected at NORDSIM under the supervision of L. Ilyinsky, K. Lindén, and M.J. Whitehouse. This is NORDSIM publication #265. The SHRIMP II facilities at Curtin University of Technology in Perth, Australia, are operated under the Perth Consortium, comprising Curtin University of Technology, the University of Western Australia and the Geological Survey of Western Australia. The facility was funded by the Australian Research Council. N. Mattielli and J. de Jong are thanked for the Pb isotope measurements on the Nu Plasma MC-ICPMS at ULB (Brussels). This is Lamont-Doherty Earth Observatory Contribution No 7470. Jean Bédard and Fernando Corfu are greatly thanked for their constructive reviews of the manuscript.

References

Andersen, T., 1997. Radiogenic isotope systematics of the Herefoss granite, south Norway: an indicator of Sveconorwegian (Grenvillian) crustal evolution in the Baltic Shield. Chemical Geology 135, 139–158.

Andersen, T., Laajoki, K., 2003. Provenance characteristics of Mesoproterozoic metasedimentary rocks from Telemark, South Norway: a Nd-isotope mass-balance model. Precambrian Research 126, 95–122.
Andersen, T., Hagelia, P., Whitehouse, M.J., 1994. Precambrian multi-stage crustal evolution in the Bamble sector of south Norway: Pb isotopic evidence from a Sveconorwegian deep-seated granitic intrusion. Chemical Geology (Isotope Geoscience Section) 116, 327–343.
Andersen, T., Maijer, C., Veschure, R.H., 1995. Metamorphism, provenance ages and source characteristics of Precambrian clastic metasediments in the Bamble sector, south Norway. Petrology 3, 321–339.
Andersen, T., Andresen, A., Sylvester, A., 2001. Nature and distribution of deep crustal reservoirs in the southwestern part of the Baltic shield: evidence from Nd, Sr and Pb isotope data on late Sveconorwegian granites. Journal of the Geological Society 158, 253–267.
Andersen, T., Andresen, A., Sylvester, A., 2002a. Timing of late- to post-tectonic Sveconorwegian granitic magmatism in South Norway. Norges geologiske undersøkelse Bulletin 440, 5–18.
Andersen, T., Griffin, W.L., Pearson, N.J., 2002b. Crustal evolution in the SW part of the Baltic shield: the Hf isotope evidence. Journal of Petrology 43 (9), 1725–1747.
Andersen, T., Graham, S., Sylvester, A.G., 2007a. Timing and tectonic significance of Sveconorwegian A-type granitic magmatism in Telemark, southern Norway: new results from laser-ablation ICPMS U–Pb dating of zircon. Norges geologiske undersøkelse Bulletin 447, 17–31.
Andersen, T., Griffin, W.L., Sylvester, A.G., 2007b. Sveconorwegian crustal underplating in southwestern Fennoscandia: LAM-ICPMS U–Pb and Lu–Hf isotope evidence from granites and gneisses in Telemark, southern Norway. Lithos 93, 273–287.
Andersson, M., Lie, J., Husebye, E., 1996. Tectonic setting of post-orogenic granites within SW Fennoscandia based on deep seismic and gravity data. Terra Nova 8 (6), 558–566.
Arndt, N., Goldstein, S., 1989. An open boundary layer between lower continental crust and mantle: its role in crust formation and crustal recycling. Tectonophysics 161, 201–212.
Ashwal, L.D., 1993. Anorthosites. Springer, Berlin, Heidelberg. 422pp.
Balling, N., 1985. Thermal structure of the lithosphere beneath the Norwegian–Danish basin and the southern baltic shield: a major transition zone. Terra Cognita 5, 377–378.
Barbarin, B., Didier, J., 1992. Genesis and evolution of mafic microgranular enclaves through various types of interaction between coexisting felsic and mafic magmas. Transactions of the Royal Society of Edinburgh, Earth Sciences 83, 145–153.
Barling, J., Weis, D., Demaiffe, D., 2000. A Sr-, Nd-, and Pb-isotopic investigation of the transition between two megacyclic units of the Bjerkreim–Sokndal layered intrusion, south Norway. Chemical Geolology 165, 47–65.
Beard, J.S., Lofgren, G.E., 1991. Dehydration melting and water-saturated melting of basaltic and andesitic greenstones and amphibolites a 1, 3, 6.9 kb. Journal of Petrology 32 (2), 365–401.
Bédard, J., 2001. Parental magmas of Nain Plutonic Suite anorthosites and mafic cumulates: a trace element modelling approach. Contributions to Mineralogy and Petrology 141, 747–771.
Bédard, J., 2010. Parental magmas of Grenville Province massif-type anorthosites, and conjectures about why massif anorthosites are restricted to the Proterozoic. Earth and Environmental Science Transactions of the Royal Society of Edinburgh-Earth Sciences 100, 77–103.
Bingen, B., 1988. Origine magmatique et évolution métamorphique de la série des gneiss oeillés de Norvège méridionale. PhD thesis, Université Libre de Bruxelles, Bruxelles, 308 pp.
Bingen, B., 1989. Geochemistry of Sveconorwegian augen gneisses from SW Norway at the amphibolite–granulite facies transition. Norsk Geologisk Tidsskrift 69, 177–189.
Bingen, B., Stein, H., 2003. Molybdenite Re–Os dating of biotite dehydration melting in the Rogaland high-temperature granulites, S Norway. Earth and Planetary Science Letters 208, 181–195.
Bingen, B., van Breemen, O., 1998a. Tectonic regimes and terrane boundaries in the high-grade Sveconorwegian belt of SW Norway, inferred from U–Pb zircon geochronology and geochemical signature of augen gneiss suites. Journal of the Geological Society, London 155, 143–154.
Bingen, B., van Breemen, O., 1998b. U–Pb monazite ages in amphibolite- to granulite-facies orthogneisses reflect hydrous mineral breakdown reactions: Sveconorwegian Province of SW Norway. Contributions to Mineralogy and Petrology 132, 336–353.
Bingen, B., Demaiffe, D., Hertogen, J., Weis, D., Michot, J., 1993. K-rich calc-alkaline augen gneisses of Grenvillian age in SW Norway: mingling of mantle-derived and crustal components. The Journal of Geology 101, 763–778.
Bingen, B., Austrheim, H., Whitehouse, M.J., 2001. Ilmenite as a source for zirconium during high-grade metamorphism? Textural evidence from the Caledonides of W. Norway and implications for zircon geochronology. Journal of Petrology 42, 355–375.
Bingen, B., Mansfeld, J., Sigmond, E.M.O., Stein, H.J., 2002. Baltica–Laurentia link during the Mesoproterozoic: 1.27 Ga development of continental basins in the Sveconorwegian Orogen, southern Norway. Canadian Journal of Earth Sciences 39, 1425–1440.
Bingen, B., Nordgulen, O., Sigmond, E.M.O., Tucker, R.D., Mansfeld, J., Hogdahl, K., 2003. Relations between 1.19–1.13 Ga continental magmatism, sedimentation and metamorphism, Sveconorwegian province, S Norway. Precambrian Research 124, 215–241.
Bingen, B., Skår, Ø., Marker, M., Sigmond, E.M.O., Nordgulen, Ø., Ragnhildsveit, J., Mansfeld, J., Tucker, R.D., Liégeois, J.-P., 2005. Timing of continental building in the Sveconorwegian orogen, SW Norway. Norwegian Journal of Geology 85 (1&2), 87–116.
Bingen, B., Stein, H.J., Bogaerts, M., Bolle, O., Mansfeld, J., 2006. Molybdenite Re–Os dating constrains gravitational collapse of the Sveconorwegian orogen. SW Scandinavia Lithos 87, 328–346.
Bingen, B., Nordgulen, O., Viola, G., 2008. A four-phase model for the Sveconorwegian orogeny, SW Scandinavia. Norwegian Journal of Geology 88, 43–72.
Bogaerts, M., Scaillet, B., Liégeois, J.-P., Vander Auwera, J., 2003a. Petrology and geochemistry of the Lyngdal granodiorite (Southern Norway) and the role of fractional crystallization in the genesis of the Proterozoic ferro-potassic A-type granites. Precambrian Research 124, 149–184.
Bogaerts, M., Scaillet, B., Vander Auwera, J., 2003b. Emplacement of the Lyngdal granodiorite (SW Norway) at the brittle–ductile transition in a hot crust. Joint EGS-EUG. Geophysical Research Abstracts. Cambridge University Publications, Nice (France), p. 03611.
Bogaerts, M., Scaillet, B., Vander Auwera, J., 2006. Phase equilibria of the Lyngdal granodiorite (Norway): implications for the origin of metaluminous ferroan granitoids. Journal of Petrology 47 (12), 2405–2431.
Bogdanova, S., Bingen, B., Gorbatschev, R., Kheraskova, T., Kozlov, V., Puchkov, V., Volozh, Y., 2008. The East European Craton (Baltica) before and during the assembly of Rodinia. Precambrian Research 160, 23–45.
Bolle, O., Duchesne, J., 2007. The apophysis of the Bjerkreim–Sokndal layered intrusion (Rogaland anorthosite province, SW Norway): a composite pluton build by tectonically-driven emplacement of magmas along the margin of an AMC igneous complex. Lithos 98, 292–312.
Bolle, O., Diot, H., Duchesne, J.C., 2000. Magnetic fabric and deformation in charnockitic igneous rocks of the Bjerkreim–Sokndal layered intrusion (Rogaland, Southwest Norway). Journal of Structural Geology 22, 647–667.
Bolle, O., Demaiffe, D., Duchesne, J.C., 2003a. Petrogenesis of jotunitic and acidic members of an AMC suite (Rogaland anorthosite province, SW Norway): a Sr and Nd isotopic assessment. Precambrian Research 124, 185–214.
Bolle, O., Diot, H., Trindade, R.I.F., 2003b. Magnetic fabrics in the Holum granite (Vest-Agder, southernmost Norway): implications for the late evolution of the Sveconorwegian (Grenvillian) orogen of SW Scandinavia. Precambrian Research 121, 221–249.
Bolle, O., Diot, H., Liégeois, J.-P., Vander Auwera, J., 2010. The Farsund intrusion (SW Norway): a marker of Late-Sveconorwegian (Grenvillian) coeval transtension and gravity-driven tectonism. Journal of Structural Geology 32, 1500–1518.
Bologne, G., Duchesne, J., 1991. Analyse des roches silicatées par spectrométrie de fluorescence-X: précision et exactitude. Professional Paper Geological Survey 249, 1–11.
Brewer, T.S., Menuge, J.F., 1998. Metamorphic overprinting of Sm–Nd isotopic systems in volcanic rocks: the Telemark Supergroup, southern Norway. Chemical Geology 145, 1–16.
Brewer, T.S., Åhäll, K.I., Darbyshire, D.P.F., Menuge, J.F., 2002. Geochemistry of late Mesoproterozoic volcanism in southwestern Scandinavia: implications for Sveconorwegian/Grenvillian plate tectonic models. Journal of the Geological Society, London 159, 129–144.
Brewer, T.S., Åhäll, K.I., Menuge, J.F., Storey, C.D., Parrish, R.R., 2004. Mesoproterozoic bimodal volcanism in SW Norway, evidence for recurring pre-Sveconorwegian continental margin tectonism. Precambrian Research 134, 249–273.
Brown, L., McEnroe, S., 2008. Magnetic properties of anorthosites: a forgotten source for planetary magnetic anomalies? Geophysical Research Letters 35, L02305.
Brueckner, H., 2009. Subduction of continental crust, the origin of post-orogenic granitoids (and anorthosites?) and the evolution of Fennoscandia. Journal of the Geological Society 166, 753–762.
Buddington, A.F., Lindsley, D.H., 1964. Iron–titanium oxide minerals and synthetic equivalents. Journal of Petrology 5, 310–357.
Cawood, P., Strachan, R., Cutts, K., Kinny, P., Hand, M., Pisarevsky, S., 2010. Neoproterozoic orogeny along the margin of Rodinia: Valhalla orogen, North Atlantic. Geology 38, 99–102.
Charlier, B., Skår, Ø., Korneliussen, A., Duchesne, J.C., Vander Auwera, J., 2007. Ilmenite composition in the Tellnes deposit: fractional crystallization, postcumulus evolution and ilmenite–zircon relation. Contributions to Mineralogy and Petrology 154 (2), 119–134.
Charlier, B., Longhi, J., Vander Auwera, J., Storme, J., Maquil, R., Duchesne, J.C., 2010. Continuous polybaric fractional crystallization of high-alumina basalt parental magmas in the Egersund–Ogna massif-type anorthosite (Rogaland, SW Norway) constrained by plagioclase and high-alumina orthopyroxene megacrysts. Journal of Petrology 51, 2515–2546.
Corfu, F., 2004. U–Pb age, setting and tectonic significance of the anorthosite–mangerite–charnockite–granite suite, Lofoten-Vesterålen, Norway. Journal of Petrology 45, 1799–1819.
Corti, G., Bonini, M., Conticelli, S., Innocenti, F., Manetti, P., Sokoutis, D., 2003. Analogue modelling of continental extension: a review focused on the relations between the patterns of deformation and the presence of magma. Earth Science Reviews 63, 169–247.
deHaas, G., Andersen, T., Vestin, J., 1999. Detrital zircon geochronology: new evidence for an old model for accretion of the SW Baltic Shield. Journal of Geology 107, 569–586.
Dekker, A.G., 1978. Amphiboles and their host rocks in the high-grade metamorphic Precambrian of Rogaland/Vest-Agder, SW. Norway. Geologica Ultraiectina, 17. Rijksuniversiteit te Utrecht, Utrecht. 277 pp.
Demaiffe, D., Hertogen, J., 1981. Rare earth element geochemistry and strontium isotopic composition of a massif-type anorthositic–charnockitic body: the Hidra massif (Rogaland, SW. Norway). Geochimica et Cosmochimica Acta 45, 1545–1561.
Demaiffe, D., Weis, D., Michot, J., Duchesne, J.C., 1986. Isotopic constraints on the genesis of the anorthosite suite of rocks. Chemical Geology 57, 167–179.

Demaiffe, D., Bingen, B., Wertz, P., Hertogen, J., 1990. Geochemistry of the Lyngdal hyperites (S.W. Norway): comparison with the monzonorites associated with the Rogaland anorthosite complex. Lithos 24, 237–250.
DePaolo, D., Linn, A.M., Schubert, G., 1991. The continental crustal age distribution: methods of determining mantle separation ages from Sm–Nd isotopic data and application to the Southwestern United States. Journal of Geophysical Research 96 (B2), 2071–2088.
Dons, J., 1960. The stratigraphy of supracrustal rocks, granitization and tectonics in the Precambrian Telemark area Southern Norway. Norges geologiske undersøkelse Bulletin 212, 1–30.
Duchesne, J.C., 1972. Iron–titanium oxide minerals in the Bjerkrem–Sogndal massif, South-Western Norway. Journal of Petrology 13, 57–81.
Duchesne, J.C., 1978. Quantitative modeling of Sr, Ca, Rb and K in the Bjerkrem–Sogndal layered lopolith (S.W. Norway). Contributions to Mineralogy and Petrology 66, 175–184.
Duchesne, J.C., 1987. The Rogaland intrusive massifs: eastern part. In: Maijer, C., Padget, P. (Eds.), The Geology of Southernmost Norway: An Excursion Guide: Norges geol. undersøkelse, Special publication no 1, pp. 63–66.
Duchesne, J.C., 1990. Origin and evolution of monzonorites related to anorthosites. Schweizerische Mineralogische und Petrographische Mitteilungen 70, 189–198.
Duchesne, J.C., Demaiffe, D., 1978. Trace elements and anorthosite genesis. Earth and Planetary Science Letters 38, 249–272.
Duchesne, J.C., Hertogen, J., 1988. Le magma parental du lopolithe de Bjerkreim–Sokndal (Norvège méridionale). Comptes rendus de l'Académie des Sciences de Paris 306, 45–48.
Duchesne, J.C., Korneliussen, A. (Editors), 2003. Ilmenite deposits and their geological environment, with special reference to the Rogaland Anorthosite Province, including a geological map at scale 1:75,000 and a CD with (the text) of a guide to the province. Norges geologisk undersøkelse, Special publication no 9, 138 pp.
Duchesne, J.C., Maquil, R., 1987. The Egersund–Ogna massif. In: Maijer, C., Padget, P. (Eds.), The Geology of Southernmost Norway: An Excursion Guide. Norges geologiske undersøkelse, Special publication no 1, pp. 50–56.
Duchesne, J.C., Wilmart, E., 1997. Igneous charnockites and related rocks from the Bjerkreim–Sokndal layered intrusion (Southwest Norway): a jotunite (hypersthene monzodiorite)-derived A-type granitoid suite. Journal of Petrology 38 (3), 337–369.
Duchesne, J.C., Roelandts, I., Demaiffe, D., Hertogen, J., Gijbels, R., De Winter, J., 1974. Rare-earth data on monzonoritic rocks related to anorthosites and their bearing on the nature of the parental magma of the anorthositic series. Earth and Planetary Science Letters 24, 325–335.
Duchesne, J.C., Maquil, R., Demaiffe, D., 1985a. The Rogaland anorthosites: facts and speculations. In: Tobi, A.C., Touret, J.L.R. (Eds.), The Deep Proterozoic Crust in the North Atlantic Province. Reidel, Doordrecht, pp. 449–476.
Duchesne, J.C., Roelandts, I., Demaiffe, D., Weis, D., 1985b. Petrogenesis of monzonoritic dykes in the Egersund–Ogna anorthosite (Rogaland, SW Norway): trace elements and isotopic (Sr, Pb) constraints. Contributions to Mineralogy and Petrology 90, 214–225.
Duchesne, J.C., Caruba, R., Iacconi, P., 1987a. Zircon in charnockitic rocks from Rogaland (southwest Norway): petrogenetic implications. Lithos 20, 357–368.
Duchesne, J.C., Michot, J., Demaiffe, D., Maquil, R., Wilmart, E., 1987b. The Rogaland intrusive masses. In: Maijer, C., Padget, P. (Eds.), The Geology of Southernmost Norway: An Excursion Guide. Norges geologiske undersøkelse, Special publication no 1, pp. 42–66.
Duchesne, J.C., Wilmart, E., Demaiffe, D., Hertogen, J., 1989. Monzonorites from Rogaland (southwest Norway): a series of rocks coeval but not comagmatic with massif-type anorthosites. Precambrian Research 45, 111–128.
Duchesne, J.C., Liégeois, J.-P., Vander Auwera, J., Longhi, J., 1999. The crustal tongue melting model and the origin of massive anorthosites. Terra Nova 11, 100–105.
Duchesne, J.C., Vander Auwera, J., Liégeois, J.-P., Barton, E., Clifford, T., 2007. Geochemical constraints on the petrogenesis of the O'okiep Koperberg Suite and granitic plutons (Namaqualand, S Africa): a lower crustal mafic source in Namaquan (Grenville) times. Precambrian Research 153, 116–142.
Duchesne, J.C., Charlier, B., Vander Auwera, J., 2008. Evolution of oxygen fugacity with crystallization in the Bjerkreim–Sokndal layered intrusion. 33th International Geological Conference, Oslo, Norway.
Dupont, A., 2003. Pétrologie, géochimie et géochimie isotopique du massif de Farsund (Norvège): implications pour le magmatisme AMCG. PhD Thesis, Université de Liège, Liège, 279 pp.
Dupont, A., Vander Auwera, J., Paquette, J.-L., Pin, C., Bogaerts, M., 2005. Inefficiency of magma mixing and source heterogeneity in the genesis of granitoids: the example of the Farsund body (southern Norway). Joint EGS-EUG: Geophysical Research Abstracts, 7, p. 04915.
Elliott, T., Zindler, A., Bourdon, B., 1999. Exploring the kappa conundrum: the role of recycling in the lead isotope evolution of the mantle. Earth and Planetary Science Letters 169, 129–145.
Emslie, R.F., 1978. Anorthosite massifs, Rapakivi granites, and the late Proterozoic rifting of North America. Precambrian Research 7, 61–98.
Emslie, R.F., 1985. Proterozoic anorthosite massifs. In: Tobi, A.C., Touret, J.L.R. (Eds.), The Deep Proterozoic Crust in the North Atlantic Provinces. Reidel, Dordrecht, pp. 39–60.
Emslie, R.F., Hamilton, M.A., Thiérault, R.J., 1994. Petrogenesis of a Mid-Proterozoic Anorthosite–Mangerite–Charnockite–Granite (AMCG) complex: isotopic and chemical evidence from the Nain plutonic suite. Journal of Geology 102, 539–558.
England, P., Thompson, A., 1986. Some thermal and tectonic models for crustal melting in continental collision zones. In: Coward, M., Ries, A. (Eds.), Collision Tectonics. Geological Society of London Special Publication, pp. 83–94.
Falkum, T., 1982. Geologisk kart over Norge, berggrunnskart Mandal — 1:250000. Norges geologiske undersøkelse.
Falkum, T., Wilson, J., Petersen, J., Zimmermann, H., 1979. The intrusive granites of the Farsund area, south Norway: their interrelations and relations with the Precambrian metamorphic envelope. Norsk Geologisk Tidsskrift 59, 125–139.
Faure, G., 1986. Principles of Isotope Geology. Wiley, New York. 589pp.
Foley, S., 1992. Petrological characterization of the source components of potassic magmas: geochemical and experimental constraints. Lithos 28, 187–204.
Fram, M., Longhi, J., 1992. Phase equilibria of dikes associated with Proterozoic anorthosite complexes. American Journal of Science 77, 605–616.
Frost, B.R., 1991. Magnetic petrology: factors that control the occurrence of magnetite in crustal rocks. In: Lindsley, D. (Ed.), Oxide Minerals: Petrologic and Magnetic Significance. Mineralogical Society of America, Washington, DC, pp. 489–506.
Frost, C., Frost, B.R., 1997. Reduced rapakivi-type granites: the tholeiite connection. Geology 25, 647–650.
Frost, B.R., Frost, C.D., 2008. A geochemical classification for feldspathic igneous rocks. Journal of Petrology 49 (11), 1955–1969.
Frost, B.R., Arculus, R.J., Barnes, C.G., Collins, W.J., Ellis, D.J., Frost, C.D., 2001. A geochemical classification of granitic rock suites. Journal of Petrology 42, 2033–2048.
Galer, S., 1999. Optimal double and triple spiking for high precision lead isotopic measurement. Chemical Geology 157, 255–274.
Grove, T., Parman, S., 2004. Thermal evolution of the earth as recorded by komatiites. Earth and Planetary Science Letters 219, 173–187.
Hamilton, M., Ryan, A., Emslie, R., Ernanovics, I., 1998. Identification of Paleoproterozoic anorthositic and monzonitic rocks in the vicinity of the Mesoproterozoic Nain Plutonic Suite, Labrador: U–Pb evidence. Radiogenic Age and isotopic Studies, Geological Survey of Canada, Current Research no. 1998-F, pp. 23–40.
Heaman, L.M., Smalley, P.C., 1994. A U–Pb study of the Morkheia Complex and associated gneisses, south Norway: implications for disturbed Rb–Sr systems and for the temporal evolution of Mesoproterozoic magmatism in Laurentia. Geochimica et Cosmochimica Acta 58, 1899–1911.
Holland, T., Babu, E., Waters, D., 1996. Phase relations of osumilite and dehydration melting in pelitic rocks: a simple thermodynamic model for the KFMASH system. Contributions to Mineralogy and Petrology 124, 383–394.
Johansson, L., Möller, C., Söderlund, U., 2001. Geochronology of eclogite facies metamorphism in the Sveconorwegian Province of SW Sweden. Precambrian Research 106, 261–275.
Knudsen, T., Andersen, T., Maijer, C., Verschure, R., 1997. Trace-element characteristics and Pb isotopic evolution of metasediments and associated Proterozoic rocks from the amphibolite- to granulite-facies Bamble sector, southern Norway. Chemical Geology 143, 145–169.
Kullerud, L., Machado, N., 1991. End of a controversy: U–Pb geochronological evidence for significant Grenvillian activity in the Bamble area, Norway. Terra Abstracts, Supplement to Terra Nova 3, 504.
Laajoki, K., Corfu, F., Andersen, T., 2002. Lithostratigraphy and U–Pb geochronology of the Telemark supracrustals in the Bandak–Sauland area, Telemark, South Norway. Norwegian Journal of Geology 82, 119–138.
Liégeois, J.-P., Navez, J., Hertogen, J., Black, R., 1998. Contrasting origin of post-collisional high-K calc-alkaline and shoshonitic versus alkaline and peralkaline granitoids. The use of sliding normalization. Lithos 45, 1–28.
Longhi, J., 2005. A mantle or mafic crustal source for Proterozoic anorthosites? Lithos 83, 183–198.
Longhi, J., Fram, M.S., Vander Auwera, J., Montieth, J.N., 1993. Pressure effects, kinetics, and rheology of anorthositic and related magmas. American Mineralogist 78, 1016–1030.
Longhi, J., Vander Auwera, J., Fram, M., Duchesne, J.C., 1999. Some phase equilibrium constraints on the origin of Proterozoic (Massif) anorthosites and related rocks. Journal of Petrology 40 (2), 339–362.
Ludwig, K., 2000. SQUID 1.00: a user's manual. Berkeley Geochronology Center Special Publication 2, 1–19.
Ludwig, K., 2003. Isoplot 3.09, a geochronological toolkit for Microsoft Excel. Berkeley Geochronology Center, Special Publication No. 4.
Lugmair, G., Marti, K., 1978. Lunar initial $^{143}Nd/^{144}Nd$: differential evolution of the lunar crust and mantle. Earth and Planetary Science Letters 39, 349–357.
Lundmark, A., Corfu, F., 2008. Late-orogenic Sveconorwegian massif anorthosite in the Jotun Nappe Complex, SW Norway, and causes of repeated AMCG magmatism along the Baltoscandian margin. Contributions to Mineralogy and Petrology 155, 147–163.
Maijer, C., 1987. The metamorphic envelope of the Rogaland intrusive complex. In: Maijer, C., Padget, P. (Eds.), The Geology of Southernmost Norway: An Excursion Guide: Norges Geologiske Undersøkelse, Special Publication No 1, pp. 68–73.
Markl, G., Hohndorf, A., 2003. Isotopic constraints on the origin of AMCG-suite rocks on the Lofoten islands, Norway. Mineralogy and Petrology 78 (3–4), 149–171.
Martin, H., 1986. Effect of steeper Archean geothermal gradient on geochemistry of subduction-zone magmas. Geology 14, 753–756.
Menuge, J., 1988. The petrogenesis of massif anorthosites: a Nd and Sr isotopic investigation of the Proterozoic of Rogaland–Vest Agder, SW Norway. Contributions to Mineralogy and Petrology 98, 363–373.
Michot, J., Michot, P., 1969. The problem of anorthosites: the south-Rogaland igneous complex, southwestern Norway. In: Isachsen, Y.W. (Ed.), Origin of Anorthosites and Related Rocks: New York State Museum and Science Service, Memoir 18, pp. 399–410.
Möller, A., O'Brien, P., Kennedy, A., Kröner, A., 2002. Polyphase zircon in ultrahigh-temperature granulites (Rogaland, SW Norway): constraints for Pb diffusion in zircon. Journal of Metamorphic Geology 20, 727–740.
Morisset, C., Scoates, J., 2008. Origin of zircon rims around ilmenite in mafic plutonic rocks of Proterozoic anorthosite suites. The Canadian Mineralogist 46, 289–304.
Morse, S., 1982. A partisan review of Proterozoic anorthosites. American Mineralogist 67, 1087–1100.

Mulch, A., Cosca, M., Andresen, A., Fiebig, J., 2005. Time scales of deformation and exhumation in extensional detachment systems determined by high-spatial resolution in situ UV-laser $^{40}Ar/^{39}Ar$ dating. Earth and Planetary Science Letters 233, 375–390.

Nagler, T., Kramers, J., 1998. Nd isotopic evolution of the upper mantle during the Precambrian: models, data and the uncertainty of both. Precambrian Research 91, 233–252.

Navez, J., 1995. Détermination d'éléments en traces dans les roches silicatées par ICP-MS. Musée Royal de l'Afrique centrale, Tervuren, Belgique, Rapport annuel 1993–1994, pp. 139–147.

Nolan, K.M., Morse, S.A., 1986. Marginal rocks resembling the estimated bulk composition of the Kiglapait intrusion. Geochimica et Cosmochimica Acta 50, 2381–2386.

Olesen, O., Smethurst, M.A., Torsvik, T.H., Bidstrup, T., 2004. Sveconorwegian igneous complexes beneath the Norwegian–Danish Basin. Tectonophysics 387 (1–4), 105–130.

Olsen, K., Morse, S., 1990. Regional Al–Fe mafic magmas associated with anorthosite-bearing terranes. Nature 344, 760–762.

Parman, S., Dann, J., Grove, T., de Wit, M., 1997. Emplacement conditions of komatiite magmas from the 3.49 Ga Komati Formation, Barberton Greenstone Belt, South Africa. Earth and Planetary Science Letters 150, 303–323.

Parman, S., Shimizu, N., Grove, T., Dann, J., 2003. Constraints on the pre-metamorphic element composition of Barberton komatiites from ion probe analyses of preserved clinopyroxenes. Contributions to Mineralogy and Petrology 144, 383–396.

Pasteels, P., Demaiffe, D., Michot, J., 1979. U–Pb and Rb–Sr geochronology of the eastern part of the South Rogaland igneous complex, southern Norway. Lithos 12, 199–208.

Pedersen, S., Konnerup-Madsen, J., 2000. Geology of the Setesdalen area, South Norway: implications for the Sveconorwegian evolution of South Norway. Bulletin of the Geological Society of Denmark 46, 181–201.

Rietmeijer, F.J., 1984. Pyroxene (re-)equilibration in the Precambrian terrain of SW Norway between 1030–990 Ma and reinterpretation of events during regional cooling (M3 stage). Norsk Geologisk Tidsskrift 64, 7–20.

Rivers, T., Corrigan, D., 2000. Convergent margin on southeastern Laurentia during the Mesoproterozoic: tectonic implications. Canadian Journal of Earth Sciences 37, 359–383.

Robins, B., Tumyr, O., Tyseland, M., Garmann, L., 1997. The Bjerkreim–Sokndal intrusion, Rogaland, south Norway: evidence from marginal rocks for a jotunite parent magma. Lithos 39, 121–133.

Rollinson, H., 2007. Early Earth Systems: A Geochemical Approach. Blackwell Publishing. 285 pp.

Rudnick, R.L., Fountain, D.M., 1995. Nature and composition of the continental crust: a lower crustal perspective. Reviews of Geophysics 33 (3), 267–309.

Rudnick, R.L., McLennan, S.M., Taylor, S.R., 1985. Large ion lithophile elements in rocks from high-pressure granulite facies terrains. Geochimica et Cosmochimica Acta 49, 1645–1655.

Ryan, B., Hamilton, M., Emslie, R., Connelly, J., 1999. Paleoproterozoic and Mesoproterozoic anorthositic and granitic plutons in the Nain–Okak region, Labrador: repetitive anorogenic magmatism, American Geophysical Union. EOS, p. S366.

Schärer, U., Wilmart, E., Duchesne, J.C., 1996. The short duration and anorogenic character of anorthosite magmatism: U–Pb dating of the Rogaland Complex, Norway. Earth and Planetary Science Letters 139, 335–350.

Schiellerup, H., Lambert, R., Prestvik, T., Robins, B., McBride, J., Larsen, R., 2000. Re–Os isotopic evidence for a lower crustal origin of massif-type anorthosites. Nature 405, 781–784.

Scoates, J.S., Chamberlain, K.R., 1997. Orogenic to post-orogenic origin for the 1.76 Ga Horse Creek anorthosite complex, Wyoming, USA. Journal of Geology 105, 331–343.

Sigmond, E.M.O., 1985. The Mandal–Ustaoset line, a newly discovered major fault zone in south Norway. In: Tobi, A.C., Touret, J.L. (Eds.), The Deep Proterozoic Crust in the North Atlantic Provinces. Reidel, Dordrecht, pp. 323–331.

Simmons, E., Hanson, G., 1978. Geochemistry and origin of massif-type anorthosites. Contributions to Mineralogy and Petrology 66, 119–135.

Sisson, T., Ratajeski, K., Hankins, W., Glazner, A., 2005. Voluminous granitic magmas from common basaltic sources. Contributions to Mineralogy and Petrology 148, 635–661.

Snyder, D., Carmichael, I., Wiebe, R., 1993. Experimental study of liquid evolution in an Fe-rich layered mafic intrusion: constraints of the Fe–Ti oxide on the T-fO2 and T-ρ paths of tholeiitic magmas. Contributions to Mineralogy and Petrology 113, 73–86.

Steiger, R., Jäger, E., 1977. Subcommission on geochronology: convention on the use of decay constants in geo- and cosmochronology. Earth and Planetary Sciences Letters 36, 359–362.

Stein, H., Morgan, J., Markey, R., Wiszniewska, J., 1998. A Re–Os study of the Suwalki Anorthosite Massif, Northeast Poland. Geophysical Journal 4, 111–114.

Stern, R., 2001. A New Isotopic and Trace-Element Standard for the Ion Microprobe: Preliminary Thermal Ionization Mass Spectrometry (TIMS) U–Pb and Electron-Microprobe Data. Geological Survey of Canada, Ottawa, Ontario, Canada. 16 pp.

Taylor, S., Campbell, I., McCulloch, M., McLennan, S., 1984. A lower crustal origin for massif-type anorthosites. Nature 311, 372–375.

Tomkins, H.S., Williams, I.S., Ellis, D.J., 2005. In situ U-Pb dating of zircon formed from retrograde garnet breakdown during decompression in Rogaland, SW Norway. Journal of Metamorphic Geology 23, 201–215.

Toplis, M., Carroll, M., 1995. An experimental study of the influence of oxygen fugacity on Fe–Ti oxide stability, phase relations, and mineral-melt equilibria in ferro-basaltic systems. Journal of Petrology 36, 1137–1170.

Vander Auwera, J., Longhi, J., 1994. Experimental study of a jotunite (hypersthene monzodiorite): constraints on the parent magma composition and crystallization conditions (P, T, fO2) of the Bjerkreim–Sokndal layered intrusion. Contributions to Mineralogy and Petrology 118, 60–78.

Vander Auwera, J., Longhi, J., Duchesne, J.C., 1998. A liquid line of descent of the jotunite (hypersthene monzodiorite) suite. Journal of Petrology 39, 439–468.

Vander Auwera, J., Longhi, J., Duchesne, J.C., 2000. The effect of pressure on D_{Sr} (plag/melt) and D_{Cr} (opx/melt): implications for anorthosite petrogenesis. Earth and Planetary Sciences Letters 178 (3–4), 303–314.

Vander Auwera, J., Bogaerts, M., Liégeois, J.-P., Demaiffe, D., Wilmart, E., Bolle, O., Duchesne, J.C., 2003. Derivation of the 1.0–0.9 Ga ferro-potassic A-type granitoids of southern Norway by extreme differentiation from basic magmas. Precambrian Research 124, 107–148.

Vander Auwera, J., Bogaerts, M., Bolle, O., Longhi, J., 2008. Genesis of intermediate igneous rocks at the end of the Sveconorwegian (Grenvillian) orogeny (S Norway) and their contribution to intracrustal differentiation. Contributions to Mineralogy and Petrology 156 (6), 721–743.

Vervoort, J., Patchett, P., Albarède, F., Blichert-Toft, J., Rudnick, R., Downes, H., 2000. Hf–Nd isotopic evolution of the lower crust. Earth and Planetary Sciences Letters 181, 115–129.

Vigneresse, J.-L., 2005. The specific case of the Mid-Proterozoic rapakivi granites and associated suite within the context of the Columbia supercontinent. Precambrian Research 137, 1–34.

Weis, D., 1986. Genetic implications of Pb isotope geochemistry in the Rogaland anorthositic complex (southwest Norway). Chemical Geology 57, 181–199.

Weis, D., Kieffer, B., Maerschalk, C., Barling, J., De Jong, J., Williams, G., Hanano, D., Pretorius, W., Mattielli, N., Scoates, J., Goolaerts, A., Friedman, R., Mahoney, J., 2006. High-precision isotopic characterization of USGS reference materials by TIMS and MC-ICP-MS. Geochemistry, Geophysics, and Geosystems 7, Q08006. doi:10.1029/2006GC001283.

Whalen, J.B., Currie, K.L., Chappell, B.W., 1987. A-type granites: geochemical characteristics, discrimination and petrogenesis. Contributions to Mineralogy and Petrology 95, 407–419.

Whitehouse, M.J., Kamber, B., 2005. Assigning dates to thin gneissic veins in high-grade metamorphic terranes: a cautionary tale from Akilia, Southwest Greenland. Journal of Petrology 46, 291–318.

Whitehouse, M., Kamber, B., Moorbath, S., 1999. Age significance of U–Th–Pb zircon data from early Archaean rocks of west Greenland — a reassessment based on combined ion-microprobe and imaging studies. Chemical Geology 160, 201–224.

Wiebe, R., 1992. Proterozoic anorthosite complexes. In: Condie, K. (Ed.), Proterozoic Crustal Evolution (Development in Precambrian Research), Amsterdam, pp. 215–262.

Wiedenbeck, M., Allé, P., Corfu, F., Griffin, W., Meier, M., Oberli, F., Von Quadt, A., Roddick, J., Spiegel, W., 1995. Three natural zircon standards for U–Th–Pb, Lu–Hf, trace element and REE analyses. Geostandards Newsletter 19, 1–23.

Williams, I., 1998. U–Th–Pb Geochronology by ion microprobe. In: McKibben, M., Shanks III, W., Ridley, W. (Eds.), Applications of Microanalytical Techniques to Understanding Mineralizing Processes: Review in Economic Geology, pp. 1–35.

Wilmart, E., Demaiffe, D., Duchesne, J.C., 1989. Geochemical constraints on the genesis of the Tellnes ilmenite deposit, southwest Norway. Economic Geology 84, 1047–1056.

Wilson, J., Robins, B., Nielsen, F., Duchesne, J., Vander Auwera, J., 1996. The Bjerkreim–Sokndal layered intrusion, Southwest Norway. In: Cawthorn, R. (Ed.), Layered Intrusions. Elsevier, Amsterdam, pp. 231–256.

Wiszniewska, J., Claesson, S., Stein, H.J., Vander Auwera, J., Duchesne, J.C., 2002. The north-eastern Polish anorthosite massifs: petrological, geochemical and isotopic evidence for a crustal derivation. Terra Nova 14, 451–460.

Zhou, X.Q., Bingen, B., Demaiffe, D., Liégeois, J.-P., Hertogen, J., Weis, D., Michot, J., 1995. The 1160 Ma old Hidderskog meta-charnockite: implications of this A-type pluton for the Sveconorwegian belt in Vest Agder (SW Norway). Lithos 36, 51–66.